EFFECT OF SIMULTANEOUS DOPING WITH Nb,Mn,Al,Bi ON THE PIEZOELECTRIC PROPERTIES OF LEAD-ZIRCONATE-TITANATE CERAMICS NEAR THE MORPHOTROPIC PHASE BOUNDARY

A thesis submitted

in partial fulfilment of the requirements

for the degree of

MASTER OF TECHNOLOGY

by

SANGITA JAMINDAR

to the

MATERIALS SCIENCE PROGRAMME
INDIAN INSTITUTE OF TECHNOLOGY , KANPUR

February,1995.

MSP- 1995- M- JAM- EFF

DEDICATED
TO
MY PARENTS

ACKNOWLEDGEMENTS

CONTENTS

LIST OF TABLES

LIST OF FIGURES

CHAPTER 1
INTRODUCTION

1.1 PIEZOELECTRICITY:

Piezoelectricity is the creation of an electric charge by the applied stress. Cady [1] defined piezoelectricity as 'electric polarisation produced by mechanical strain in crystals belonging to certain classes, the polarisation being proportional to the strain and changing sign with it'. Two effects are observed in piezoelectricity — the direct and the converse. The direct effect is the creation of an electric charge by the application of stress on the piezoelectric solid. In terms of dielectric displacement 'D' (charge Q per unit area) and stress 'T' we may write

$$D = \frac{Q}{A} = dT \quad \text{(d expressed in coulombs/Newton)} \qquad 1.1$$

The converse effect is manifested when an applied field 'E' produces a proportional strain 'S', expansion or contraction depending on the polarity.

$$S = dE \text{ (d expressed in meters/volt)} \qquad 1.2$$

For both effects, the proportionality constant is the piezoelectric constant 'd' which is numerically identical in both cases.

$$d = \frac{D}{T} = \frac{S}{E} \qquad 1.3$$

Non-centrosymmetry is the essential condition for piezoelectricity with only one exception. 21 out of the 32 crystal classes are non-centrosymmetric. 20 out of 21 crystal classes show piezoelectricity. The single exception is (432) class of crystals. A further subgroup can be made, consisting of those ten classes which contain a unique polar axis (an electric dipole moment) in the unstrained condition. This is the pyroelectric

subclass, Fig. 1.1 summarises the interrelationship of piezoelectrics and subgroups on the basis of internal crystal symmetry.

1.2 PIEZOELECTRIC CONSTANTS :

The piezoelectric constant 'd' which relates the dielectric displacement 'D' to the strain 'S' is probably the most fundamental for conveying the concept of piezoelectricity. Another frequently used piezoelectric constant is 'g' which gives the field produced by stress and is known as piezoelectric voltage coefficient,

$$g = \frac{E}{T} = \frac{S}{D} \left[\frac{\text{Volt/meter}}{\text{Newton/Sq. Meter}} = \frac{\text{Volt/meter}}{\text{Newton}} \right] \qquad 1.4$$

The 'g' constant is related to the 'd' constant by the permittivity.

$$g = \frac{d}{\varepsilon'} = \frac{d}{K\varepsilon_0} \qquad 1.5$$

'K' is the relative dielectric constant of the material.

Additional piezoelectric constants which are only occasionally used are 'e' which relates stress 'T' to field 'E', and 'h' which relates strain 'S' to field 'E'.

$$T = -eE \qquad 1.6$$

$$E = - hS \qquad 1.7$$

Rigorous development of these relationship may be found elsewhere [2]. Jaffe [4] defined the piezoelectric constants as partial derivatives evaluated at constant stress (subscript T), constant field (subscript E), constant displacement (Subscript D) or constant strain (Subscript S). These boundary conditions can be thought of as 'free', 'short circuit', 'open circuit' and 'clamped' respectively. The actual definitions are

$$d = \left(\frac{\partial S}{\partial E} \right)_T = \left(\frac{\partial D}{\partial T} \right)_E \qquad 1.8a$$
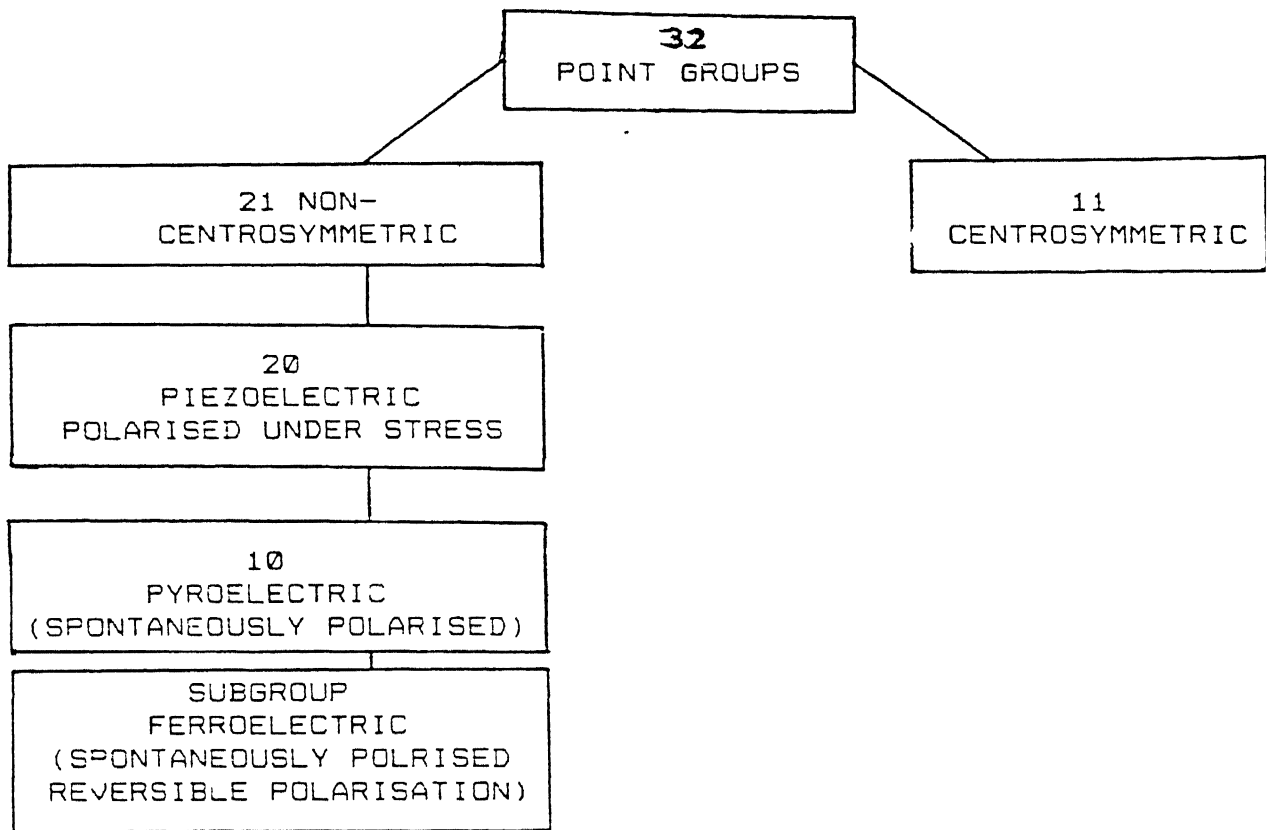
Figure 1.1 : Interreltionship of piezoelectrics crystals and
              subgroups on the basis of internal crystal
              symmetry

$$g = \left[-\frac{\partial E}{\partial T} \right]_D = \left(\frac{\partial S}{\partial D} \right)_T \qquad 1.8b$$

$$e = \left[-\frac{\partial T}{\partial E} \right]_S = \left(\frac{\partial D}{\partial S} \right)_E \qquad 1.8c$$

$$h = \left[-\frac{\partial T}{\partial D} \right]_S = -\left(\frac{\partial E}{\partial S} \right)_D \qquad 1.8d$$

The equations of state relating the electric and elastic variables can be written in a general form as follows:

$$D = dT + \varepsilon^T E \quad \text{(Direct piezoelectric effect)} \qquad 1.9$$

$$S = s^E T + dE \quad \text{(Converse piezoelectric effect)} \qquad 1.10$$

The elastic, dielectric and piezoelectric properties are orientation dependent in all piezoelectric media. For the symmetry of ceramics (α mm), the general equation is replaced by a specific set of equations.

$$D_1 = \varepsilon_1 E_1 + d_{15} T_5 \qquad 1.11a$$

$$D_2 = \varepsilon_1 E_2 + D_{15} T_4 \qquad 1.11b$$

$$D_3 = \varepsilon_3 E_3 + d_{31}(T_1 + T_2) + d_{33} T_3 \qquad 1.11c$$

$$S_1 = S_{11}^E T_1 + S_{12}^E T_2 + S_{13}^E T_3 + d_{31} E_3 \qquad 1.12a$$

$$S_2 = S_{11}^E T_2 + S_{12}^E T_1 + S_{13}^E T_3 + d_{31} E_3 \qquad 1.12b$$

$$S_3 = S_{13}^E (T_1 + T_2) + S_{33}^E T_3 + d_{33} E_3 \quad \text{(Converse effect)} \qquad 1.12c$$

$$S_4 = S_{44}^E T_4 + d_{15} E_2 \qquad 1.12d$$

$$S_5 = S_{44}^E T_5 + d_{15} E_1 \qquad 1.12e$$

$$S_6 = S_{66} T_6 \qquad 1.12f$$

The subscript 3 refers to the poling axis and 1 and 2 refer to arbitrarily chosen orthogonal axes in the plane normal to 3. Subscript 4, 5 and 6 refer to the shear stress and strain in planes normal to the 1, 2, and 3 axes, respectively. Also, by conventional notation, the first subscript of the 'd' constant gives the electrical direction (field or electric displacement)

while the second gives the component of mechanical deformation.

Another constant which gives the measurement of the strength of a piezoelectric effect is the electromechanical coupling factor k. When an electric field is applied it measures the fraction of the electrical energy converted to mechanical energy (or vice versa when a crystal or ceramic is stressed).

The actual relationship is interms of k^2.

$$k^2 = \frac{\text{Electrical energy converted to mechanical energy}}{\text{Input electrical energy}}$$

or

$$k^2 = \frac{\text{Mechanical energy converted to electrical energy}}{\text{Input mechanical energy}}$$
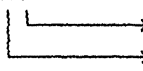
As the conversion is always incomplete the value of k is always <1. Typical values of k are 0.1 for quartz, 0.4 for barium titanate ceramic, 0.3 ~ 0.7 for Pb $(Zr_x Ti_{1-x})O_3$, 0<x<1, and as high as 0.9 for Rochelle salt at its curie point ($24^\circ C$).

Dielectric constant is another important property of these materials. The relative dielectric constant, K, or $\varepsilon/\varepsilon_0$ is the ratio between the charge stored on an electrode of this material brought to a given voltage and the charge stored on a set of identical electrodes separated by vacuum. The relative dielectric constant is dimensionless quantity. It depends on the orientation of grains of piezoelectric materials and differs widely when measured parallel or perpendicular to the polar axis [1]. The dielectric constant when measured at constant stress is called 'free' dielectric constant denoted by superscript 'T' and when measured under constant strain is known as 'clamped' dielectric constant denoted by superscript 'S'. The free and clamped dielectric constant may differ greatly for strong piezoelectric materials. The relation between the two is

$$K^S = K^T(1 - k_p)^2 \qquad\qquad 1.13$$

where k_p is electromechanical coupling coefficient (planar).

A convenient method [3] of uniquely specifying all these directional properties is to use subscripts which defines orientation direction as described in Fig. 1.2. Coefficients that relate two variables (e.g. the 'd' constant) are indicated with two subscripts, the first of which refers to the electrical direction (electric field or dielectric displacement) and the second to the mechanical direction (stress or strain). Also when a property is being measured holding another quantity constant, a superscript symbol is used to indicate the quantity held constant. The mostly used piezoelectric coefficients with appropriate subscripts and superscripts are given below:

d_{31}
    └────→ Stress or strain direction
    └────→ Displacement or electric field direction
    (electrodes are perpendicular to the '3' axis)

S^E = Compliance at constant electric field (electrodes shorted).

S^D = Compliance at constant displacement (open circuit).

ε^T = Dielectric constant at constant stress (free).

ε^S = Dielectric constant at constant strain (clamped).

K^T = Relative dielectric constant at constant stress (free).

K^S = Relative dielectric constant at constant strain (clamped).

d_{33} = Charge or strain coefficient (longitudinal); (Charge density/ applied stress, c/N; strain developed / applied field, m/V).

d_{31} = Charge or strain coefficient (lateral), m/V or c/N.

S_{31} = Mechanical compliance (lateral) m^2/N.
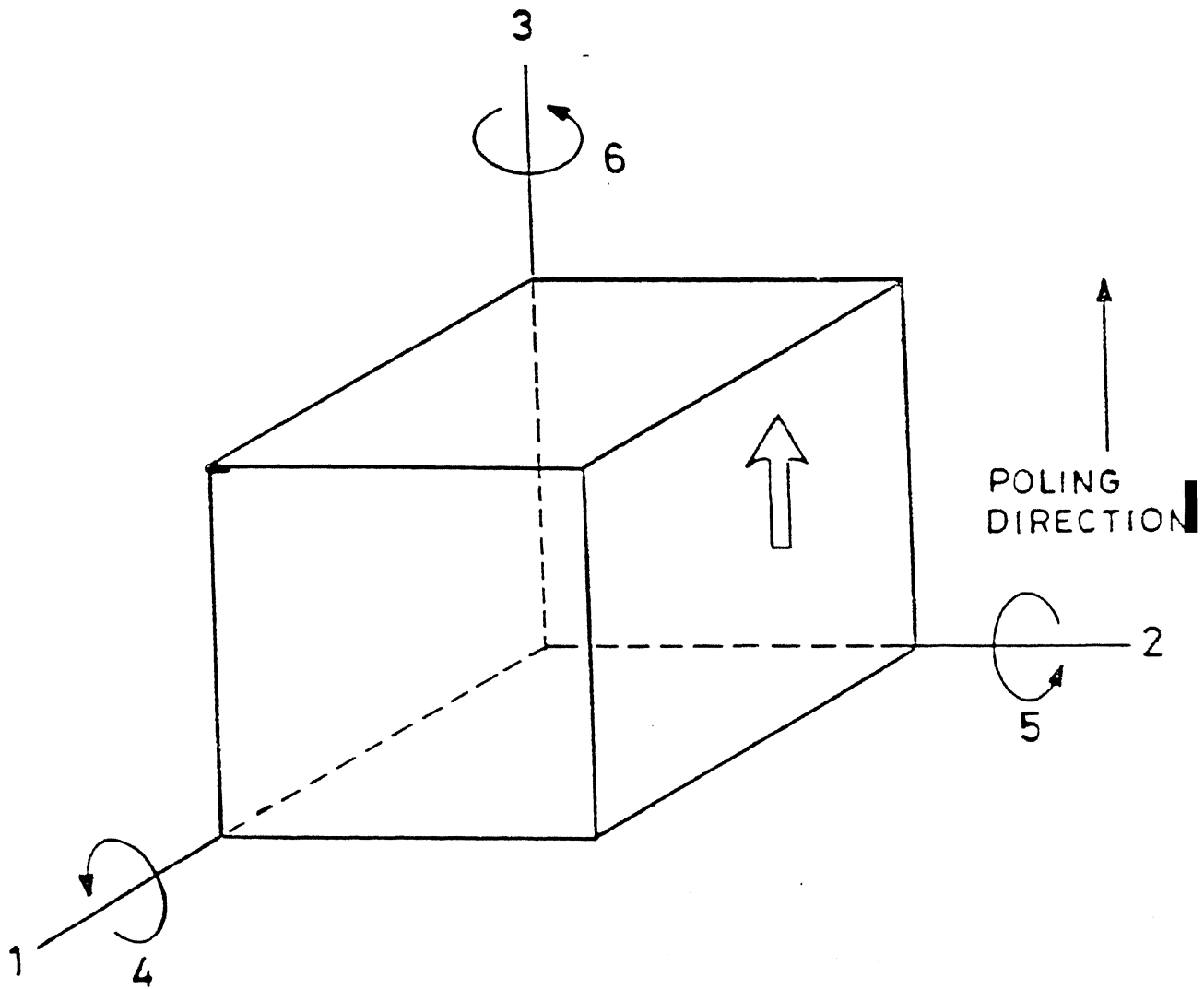
Fig. 1.2 Notation of axis for poled ceramic element.

g_{31} = Voltage coefficient (lateral), V-m/N (Open circuit field/applied stress).

K_3 = Relative dielectric constant, longitudinal, no units (K_3 = K_{33} = $\varepsilon_{33}/\varepsilon_o$)

k_{33} = Electromechanical coupling factor(longitudinal), no units.

k_{31} = Electromechanical coupling factor (lateral), no units.

k_p = Electromechanical coupling factor, planar (radial), no units (thin disk only).

Q_m = Mechanical quality factor.

Both static and dynamic methods of measurement are used to evaluate the various piezoelectric constants. A scheme for such measurements can be obtained from Appendix 1.

The details are provided in [4]. Only the resonance method has been included here to emphasise its superiority over other methods of measurement.

Simple measurements of resonant and antiresonant frequencies are used to evaluate piezoelectric effects. Elastic bodies show numerous resonances, the most pronounced are those where the body can just accommodate one half wave length of a standing elastic wave. The piezoelectric effect is a convenient way to excite such elastic waves, to permit observation of the interaction of the mechanical resonance with the electric behaviour. This is best seen in the equivalent circuit idealised for a single resonance (Fig. 1.3). The values of L_1 and C_1 are such that at the resonant frequency 'fr' the impedances $2\pi frL_1$ and $-1/2\pi frC_1$ are opposite in sign and equal in magnitude, and the total impedance of this branch is given only by the mechanical resistance 'R$_1$', which is
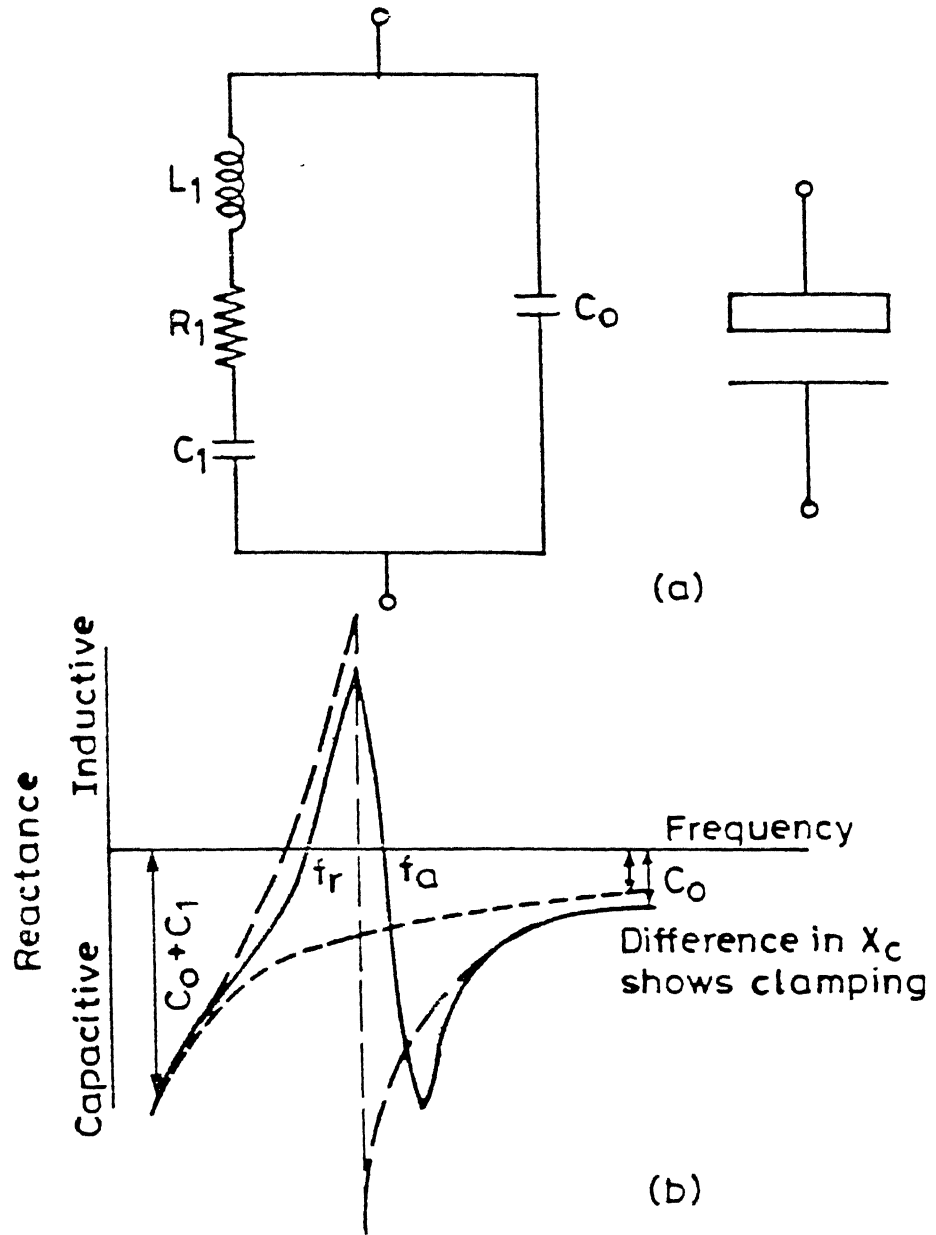
Fig.1.3 (a) Equivalent circuit of a piezoelectric body
(b) Reactance of piezoelectric resonator.

comparatively quite small. This mechanical branch is however in parallel with the electric capacitance 'Co'. The frequency of minimum impedance of 'resonance', 'fr' is that of a standing wave under 'zero field' conditions. For applied frequencies above 'fr' the mechanical branch becomes inductive. When the series impedance of this branch becomes opposite and equal to the impedance of 'Co', the impedance of the crystal reaches a maximum since opposite currents flow in the two branches. This conditions of parallel resonance, however means constant charge on the crystal. The frequency of maximum impedance or 'antiresonance' 'fa', is therefore that of a standing wave under open-circuit conditions.

1.3 LEAD-ZIRCONATE – TITANATE (PZT) SYSTEM :

The most important piezoelectric ceramics (PZT) crystallise in the Perovskite structure. This structure may be described as a simple cubic unit cell with a large cation (A) $[Pb^{+2}, Zr^{+4}]$ on the corners, a smaller cation (b) in $[Ti^{+4}]$, the body center, and oxygen (O) in the centres of the faces [Fig. 1.4]. The structure is a network of corner linked oxygen octahedra with the smaller cation filling the octahedral holes and the larger cation filling the dodecahedral holes [4]. A wide variety of cations can be substituted in the perovskite structure [5]. The relationship

$$t = (R_a + R_o)/ \sqrt{2} (R_B + R_O) \qquad\qquad 1.14$$

describes the ideal perovskite structure where t = 1.0 and R_A, R_B and R_O indicate the ionic radius of the large cation, small cation and anion respectively. In practice those structures whose tolerance factor t = 0.95 to 1.0 are cubic; those with lower t values are slightly distorted but nonferroelectric.
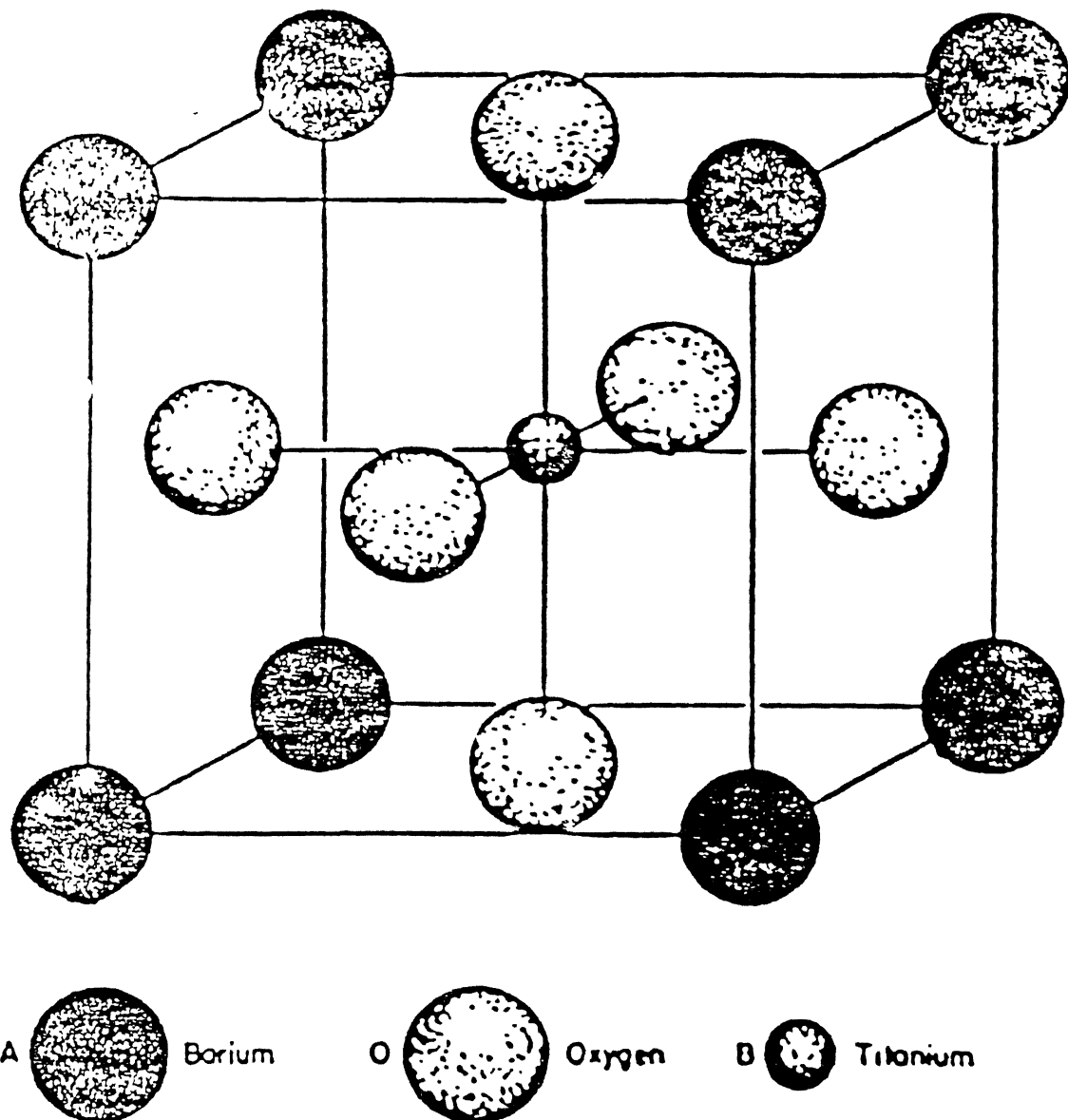
Fig. 1.4   The perovskite structure as typified by $BaTiO_3$ above its Curie point.

Polarisability of the ions is also an influential parameters. While considering this 'hardsphere' model of ion in contact, it is also necessary to consider that the bonding is not necessarily completely ionic.

The discovery of very strong and stable piezoelectric effect in PZT solid solution [6] in 1954 gave a jolt to the researchers in this field. Higher curie temperature of PZT (360°C) over $BaTiO_3$ (120°C) gave stable piezoelectric properties over a wide range of temperature.

PZT is a solid solution of lead-zirconate (rhombohedral) and lead-titanate (tetragonal) with varying degree of composition. The generalised chemical formula is $Pb(Zr_xTi_{1-x})O_3$ where $0 < x < 1$.

Esturo Sawaguchi [7] first developed the phase diagram of the solid solution of $PbZrO_3 - PbTiO_3$ system. He established that substitution of Zr^{+4} for Ti^{+4} in $PbTiO_3$ reduce the tetragonal distortion [Fig. 1.5] and ultimately causes the appearances of another ferroelectric phase of rhombohedral (R.3m) symmetry. The boundary between tetragonal and rhombohedral phases is nearly independent of temperature (morphotropic). The current version of phase diagram [Fig. 1.6] is determined with zirconia containing low amount of hafnia.

P. Ari-Cur and L. Benguigui [8] showed by means of X-ray diffraction the co-existance region to be a wide range of composition. Initially, it was thought that tetragonal - rhombohedral phase boundary (MPB) corresponds to a specific composition.

The solid state reactions leading to the formation of PZT solid solution have been studied by many investigators but with
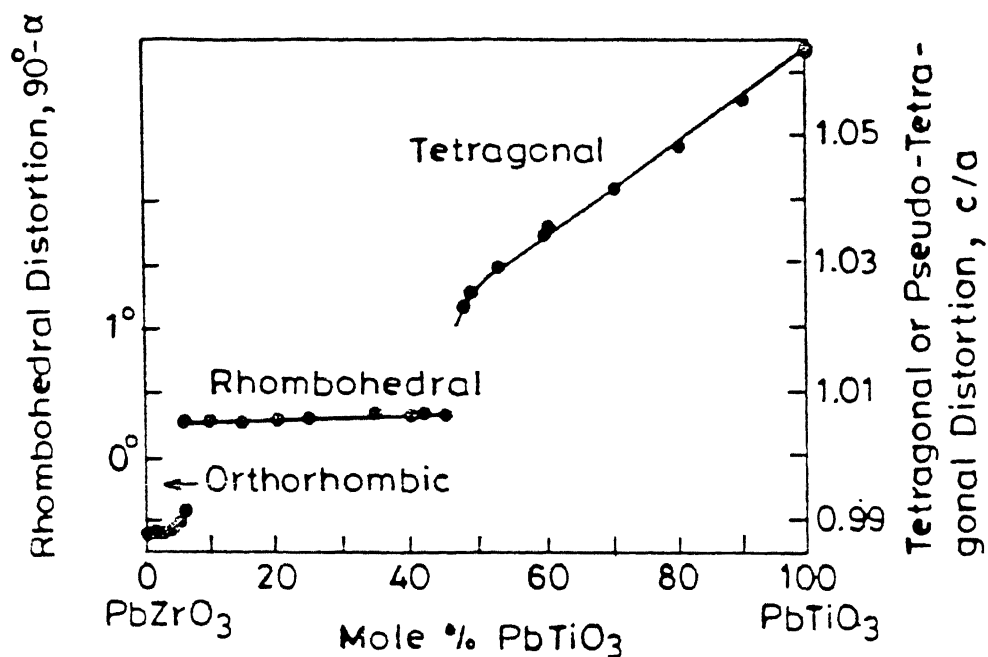
Fig. 1.5 Unit cell distortion at room temperature for the PbTiO₃ -PbZrO₃ system.
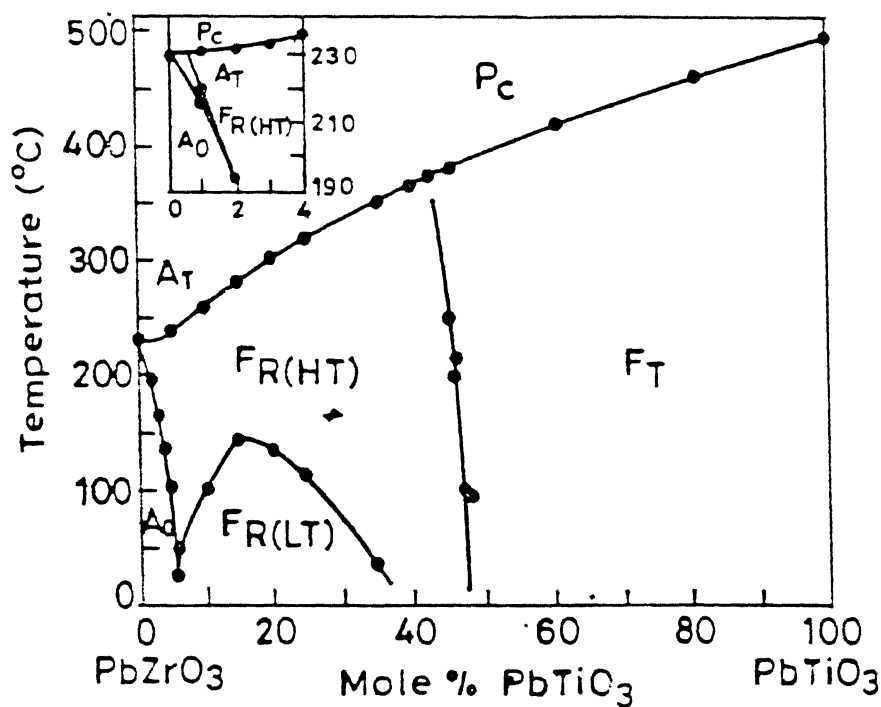
Fig. 1.6 PbTiO₃ -PbZrO₃ sub-solidus phase diagra

differing conclusions. According to Matsuo and Sasaki [9] when PbO, TiO_2 and ZrO_2 in the molar ratio 2:1:1 is heated; PbO and TiO_2 react to form $PbTiO_3$ almost completely at $650^\circ C$. The reaction $PbTiO_3 + PbO + ZrO_2 \longrightarrow Pb\ (Zr_x Ti_{1-x})\ O_3$ starts near $650^\circ C$. In this reactions soon as ZrO_2 starts to react with PbO, $PbTiO_3$ reacts to form $Pb(Zr_x Ti_{1-x})O_3$ solid solution.

The PZT ceramics offer good piezoelectric properties over a wide range of compositions. Jaffe et al [6] reported the excellent performance of PZT ceramics with compositions near the MPB. They observed high value of dielectric constant and coupling coefficient as well as relatively small variation of these with changing temperature. Composition which lies in the MPB region is of particular commercial interest.

1.4 EFFECTS OF IMPURITY DOPING IN PZT CERAMICS :

Lead zirconate titanate, $Pb(Zr, Ti)O_3$, ceramics are excellent piezoelectric materials. Their properties can be improved by doping with a small quantity of additive oxides. These dopant atoms either replace partially the constituents atoms or they make pseudoternary solid solution compounds. Properties can be further tailored with multiple oxide dopings.

B. Jaffe [4] suggested that most of impurity atoms enter into the lattice points to a certain extent and thus the ceramic piezoelectric properties change. Depending on the substitution of cations in ABO_3 perovskite type structure of PZT, the dopants or modifiers have been classified as,

i.   Insolvent cation substitution type

Example : A site (Pb^{2+}) substitute by Sr^{2+}, Ba^{2+}

ii.   Donor type

Example A site La^{3+}, Bi^{3+}, Th^{4+}

B site : Nb^{5+}, Sb^{5+}, Ta^{5+}, W^{6+}, Mo^{6+} etc.

iii. Acceptor type

A site : K^{+}, Na^{+}

B site : Mg^{2+}, Sc^{3+}, Fe^{3+}, Al^{3+}, Cr^{3+} etc

Ion valences of the acceptor atoms are lower than those of the constituent atoms. Thus oxygen vacancies are introduced for valence compensation. Ceramics doped with acceptor atoms have following properties:

1. Relatively low dielectric constant.

2. Low dielectric loss.

3. Moderately lowered electrical resistivity.

4. High mechanical quality factor.

5. High coercive field.

6. More difficult poling and depoling.

7. Relatively dark color.

8. Relative insensitivity to darkening by light.

Donors produce variances in Pb-sites, because their ion valences are higher than those of the constituent atoms. Ceramics doped with donors have a different set of properties that are

1. Increased dielectric constant.

2. High dielectric loss.

3. Increased elastic compliance.

4. Low mechanical Q.

5. High piezoelectric coupling factor.

6. Low coercive field, relatively square hysteresis loops.

7. Greatly increased electrical volume resistivity.

8. Anomalously small aging effects.

9. Easy non elastic mechanical deformation.

10. Yellow color.

11. Translucency.

12. Easy phototropic darkening.

The acceptor substituents thus have opposite effects from those of the donor substituents.

It is difficult to assign valencies to Cr and U additives [4] in Pb(Ti, Zr) O_3 ceramics. The properties suggest that these atoms are present in the lattice in more than one valence state. The properties of the ceramics are partially those of the donor doped and partially those of the acceptor doped ceramics. The following characteristics are noted for Uranium doped PZT ceramics,

1. Low aging (sometimes negative)

2. High resistivity at elevated temperature.

3. Slightly more conductive at room temperature than unmodified composition.

4. Mechanical Q very high for rhombohedral compositions.

5. Dissipation factor (1KHz) high.

6. Coupling factor normal.

and for chromium doped the properties are,

1. Low aging.

2. Resistivity slightly lowered.

3. Mechanical Q slightly high.

4. Dissipation factor (1KHz) high.

5. Reduced coupling factor.

6. Relatively low dependence of $1/S_{11}^E$ on temperature for selected compositions.

Many of the properties of donor doped PZT materials are explained on the basis of A site vacancies facilitating domain boundary motion. Domain walls can be displaced with very small electric field or mechanical stresses. This increases both elastic and dielectric compliance and loss factor. The easy wall motion greatly facilitates initial stress relief. This explains the low aging rates, since those domains under stress switch to relieve most of the stress immediately upon removal of the field. The case of switching is related to relatively low coercive field and squareness of hysteresis loops.

In the case of acceptor doped PZT materials vacancies in the Oxygen position will tend to shrink the cell size. This shrinkage and distortion of the cells by Oxygen vacancies is responsible for increasing the mechanical quality factor, high coercive force and for lowering dielectric constant.

Thus domain wall motions control many important properties. Poling process takes place owing to the domain wall motions. Mechanical quality factor depends on the domain wall hysteresis loss. Aging effect is also due to the gradual domain wall motions. Internal bias field which is controlled by impurity doping, has an influence on the domain wall motions.

An asymmetric DE hysteresis loop in poled $BaTiO_3$ ceramics is observed by investigators and they proposed the existence of an internal bias field, presumably arising during the aging process. Subsequently the same phenomenon has been found in $Pb(Zr,Ti)O_3$ ceramics by Takahashi [10]. Properties like mechanical quality factor and the aging change in frequency constant and also dielectric constant are affected by the internal bias field [11]

controlled with various single impurity additives in $Pb(Zr,Ti)O_3$ ceramics.

One of the most important properties of piezoelectric resonators is its mechanical quality factor. Mechanical quality factor depends on the various impurities present in lead zirconate ceramics. Qm is defined as the reciprocal of internal friction [12]. Acceptor Oxides such as Fe_2O_3, Cr_2O_3 and IrO_2 added to $Pb(Zr, Ti)O_3$ ceramics in a small amount, were found to increase the values of Qm. However, donor oxides such as La_2O_3, Nb_2O_5, ThO_2, WO_3, Bi_2O_3 and Sb_2O_3 decrease the values of Qm.

Decrease of Qm can be explained by the following proposed mechanism. Impurities, which create vacancies in Pb position reduces the local stress in the domains which can therefore undergo domain switching easily. As a result the domain walls become remarkably mobile and produce only micro-hysteresis. It also suggests that Qm decreases with increase of internal friction and hysteresis.

In the other case, that of acceptor doping, increase of Qm can be explained by the presence of large amount of space charge, most probably due to the oxygen vacancies, which suppresses the domain wall motion and decreases the internal friction.

The amount of space charge can be estimated [10] by an observable parameter which is defined to be the reduced amount of space charge $(P_s - P_1)/P_s$, where P_s = the value of saturated polarisation and P_1 = the value of polarization determined by the hysteresis curve obtained just after the application of an a.c. field. The values of $(P_s - P_i)/P_i$ vary with the kind and amount of impurities. Poling efficiency was found to decrease with the

increase of $(P_s-P_1)/P_s$ and the lowering of poling temperature.

Qm can be determined by means of the piezoelectric resonance with a radial fundamental mode. In accordance with appropriate IRE standards, the values of Qm can be determined by the measurements of resonance frequency fr, antiresonance frequency fa, resistance at resonance R and capacitance C. Thus values of Qm is obtained by means of the relation given below,

$$Q_m = \frac{fa^2}{2\pi fr(fa^2-fr^2)RC} \qquad 1.15$$

where the value of C is determined at 1KHz.

Specific resistivity (ρ) has been measured applying a dc field of 10oV/mm to ceramics. Sadayuki Takahashi and M. Takahashi have shown [12] the variation of mechanical quality factor Qm of $Pb(Zr_{0.52}Ti_{0.48})O_3$ ceramics containing various kinds and amounts of impurities with a reduced amount of space charge.

They found that the values of Qm increases linearly with $(P_s-P_1)/P_s$ at constant specific resistivity. These are mainly applicable to the impurities of acceptor type.

Electromechanical properties of piezoelectric materials can be improved by doping with impurities in order to meet the requirements for particular applications. It is said that some of the doping effects on the electromechanical properties are due to an internal bias field controlled by impurity doping. S. Takahashi has studied the impurity doping effects on $Pb(ZrTi)O_3$ ceramics from the internal bias field view point.

Ferroelectric DE hysteresis loop is symmetric with respect to the origin for usual ferroelectric as shown in Fig 1.7(a). If a d.c. bias field E_b is super imposed on a measuring a.c. field, the

loop is displaced asymmetrically with respect to the origin by E as shown in Fig 1.7(b) below. The loop becomes like that of Fig 1.7(b) for some ferroelectric ceramics, although no d.c. bia field has been superimposed. It appears as if the d.c. bias fiel exists naturally inside of such ceramics. This field is define as the internal bias field E_i. Thus the E_i value can b determined from the hysteresis loop.

1.5 IMPURITY DOPING EFFECTS ON INTERNAL BIAS FIELD

According to S. Takahashi [11] internal bias is strengthened by doping with the following impurity atoms, Fe, Ni, Co, Ga, In, Cr, Rh, Ir or U, but weakened by La, Nb, Ta, Sb, Bi, Th or W. Among these atoms, Fe, Ni,Co, Ga, and In are known as acceptors and those which weakened the internal bias field are known as donors. Rh and Ir atoms behave like Cr and U atoms present in the ceramics. S. Takahashi [11] selected the impurity atom K, Fe for acceptor group, La, Nb for donor group and Cr for remainder(ie partially acceptor and partially donor) and examined the doping effects on the internal bias field.

The internal bias field (Ei) value increases with increasing doping concentration (x) for K or Fe while it decreases slightly for La and Nb. For Cr doped ceramics E_i increases with x when x is less than 0.5 at %, but decreases when x is more than 0.5 at %. This decrease may be due to the internal bias field relaxation during the course of switching. In the case of multiple impurity doping it was found that doping with same kind of dopant gave rise to effects similar to those in single impurity doping. Also equimolar mixed doping of acceptor and donor seems to exert no influence on the Ei value.
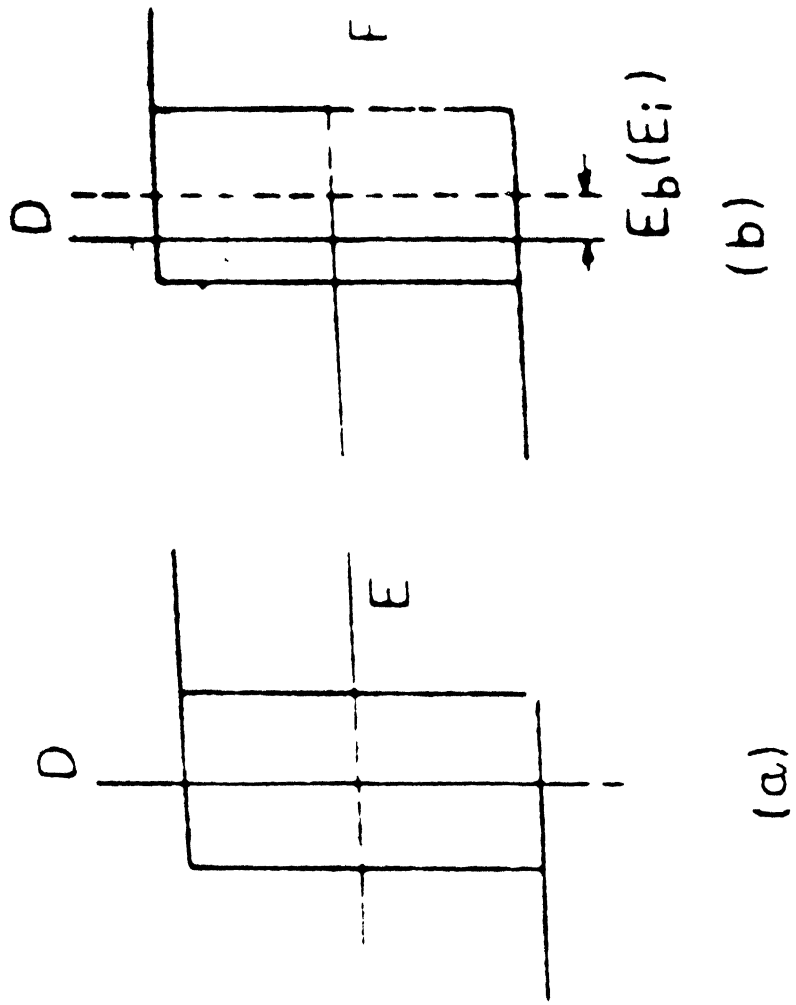
FIG. 1.7   Schemes of ferroelectric DE hysteresis

(a) Normal, (b) dc bias E_b is superimposed

1.6 INTERNAL BIAS FIELD ORIGIN

Lambeck and Jonker [13,14] found that, in reduced Mn-doped $BaTiO_3$ crystals, Mn^{+2} ions substituted for Ti-sites and Oxygen vacancies form complex with dipole character. In this case dipoles gradually orient themselves parallel to the spontaneous polarisation Ps and thus they stabilizes the polarisation. For PZT ceramics, acceptor doped atoms create, oxygen vacancies by valence compensation. Thus as in the case of $BaTiO_3$ doped with Mn^{+2}, here complexes of acceptor ions and induced vacancies stabilize the spontaneous polarisation and are the origin of internal bias field.

But according to S. Takahashi [11], Oxygen vacancies introduced by acceptor doping move slowly to the domain walls by diffusion, they pin the walls and stabilize the domains. This also leads to asymmetry in the switching current. At present it is certain that only acceptor doping is responsible for the generation of the internal bias field. Experiment shows that donors are ineffective in generating an internal bias field and are also ineffective in stabilizing the polarization. This is because they produce Pb-sites vacancies, which facilitates motion of the domain walls under electrical or mechanical drive. Internal bias field is little changed in the case of doping with equal amounts of acceptor and donor [15] from that in undoped ceramics.

Impurity doping also effects the poling process. This was examined from the internal bias field view point. Thus from the DE hysteresis loop domain wall motion under a strong electric field can be found out. DE hysteresis loops for modified PZT

ceramics doped with a single impurity like 5 at% K, 0.8 at% Fe, 2.4 at%La, 2.4 at% Nb and 0.53 at% Cr and also loop for undoped PZT are shown in Fig. 1.8. The loops were observed at room temperature by applying a 50 HZ a.c. field with 4 KV/mm peak value. The undoped and donors doped PZT show saturated normal loops just after applying the field, but the acceptors doped PZT show unsaturated constricted loops for a long time. For Cr-doped PZT, a constricted loop is obtained just after applying the field. Then, the loop changes into a saturated normal one in a short time. The unsaturated constricted loop may be due to the existence of the internal bias field.

The change in the loop during the application of the field is due to the internal bias field relaxation. Relaxation time constant for the internal bias field is smaller for Cr-doped ceramics than for acceptor doped ceramics. Thus from this it can be expected that because of the strengthened internal bias field, domain wall movement is difficult in the acceptor doped PZT. Domain walls move easily in undoped and donor doped PZT even by a d.c. field application. As poling is carried out accompanying the domain wall motions so internal bias field effects on poling process.

Also mixed impurity doping effects on mechanical quality factor Qm and aging change in frequency constant Nr. The experimental results [16] of doping effects on the properties of ceramics are summarized in Table 1.1:
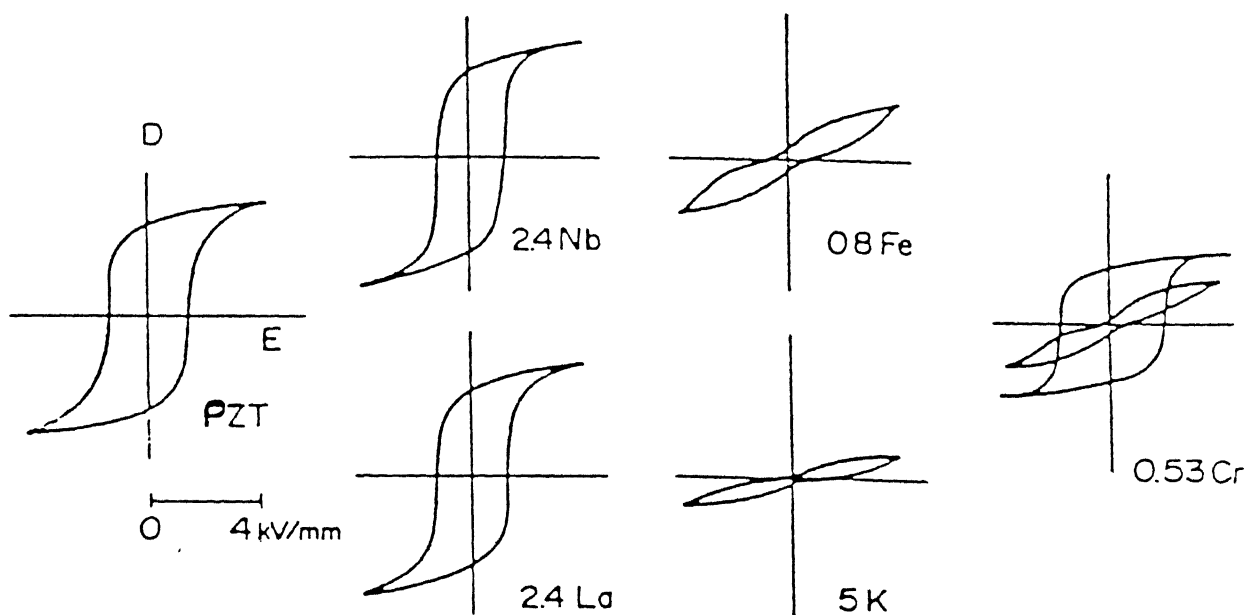
FIG. 1.8   DE hysteresis loops for Pb $(Zr_{0.52}Ti_{0.48})O_3$
ceramics doped with single impurity

Table 1.1 : Doping effects on the electromechanical properties of ceramics

Dopant	E_1	Q_m	$\Delta Nr/Nr$	ρ	ε_{33}^T	K_r
a	I	I	I	D	ID	ID
d	D	D	D	I	ID	ID
a+a	I	I	I	D	ID	ID
d+d	D	D	D	I	ID	ID
a+d (a>d)	I	I	I	D	ID	ID
a+d (a=d)	UC	UC	UC	UC	ID	ID
a+d (a<d)	D	D	D	I	ID	ID
PFN	UC	UC	UC	UC	ID	ID
PFN+a	I	I	I	D	ID	ID
PFN+d	D	D	D	I	ID	ID

where Base material : $Pb(Zr_{0.52}Ti_{0.48})O_3$

Dopant : a : acceptor (K or Fe), d : donar (La or Nb)

PFN : $Pb(Fe_{1/2}Nb_{1/2})O_3$

Symbol for doping effect : I : increase; D : decrease; UC. : unchange; ID : increase or decrease.

It is obvious that Q_m and the aging change are closely correlated with the internal bias field E_1. As for the other quantities there seems to be no correspondence with E_1.

In Ferroelectric ceramics, the mechanical loss Q_m^{-1} is mainly due to dielectric loss, so Q_m is linearly related to tan δ through electromechanical coupling. On the other hand, dielectric tan δ is the sum of macro-hysteresis loss, micro-hysteresis loss and intrinsic dielectric loss. The internal bias field reduces the hysteresis loss, through prohibiting domain wall motions.

1.7 LOW AMPLITUDE APPLICATIONS

Before discussing the principles of piezoelectric materials in electric wave filters certain points in terminology need clarifying. According to J.M. Herbert [17] 'band width' of a filter is the range of frequencies it will allow to pass with minimal attenuation. For a resonating body it is the difference between the frequency giving maximum reactance (antiresonance) and that giving minimum reactance (resonance) and is proportional to k^2. The sharpness of the impedance/frequency peak in the neighborhood of resonance is controlled by the losses in the material. The losses are due to both mechanical and electrical causes but mechanical loss is taken as the dominant factor near resonance and is usually expressed by its inverse, Qm (Q=1/tan δ). Qm can be determined from the width, Δf, of the impedance/frequency peak at an impedance level which is equal to the maximum impedance divided by root two, i.e. Qm = fr/Δf where fr is the resonant frequency. Thus k and Qm are the important parameters determining the impedance/frequency characteristics of resonating systems and the term band width may apply, in different senses to both of them. In what follows 'band width' is the frequency interval associated with k.

Solid bodies can be excited into a wide range of vibrational modes by suitable excitation [17]. If the excitation is provided by a piezoelectric transducer energy will be transferred to the body most effectively at its resonant frequency. A second transducer may be used to convert the mechanical vibration back into an electrical signal and the transfer of the signal from one transducer to the other will only occur efficiently at the

resonant frequencies of the intermediate body. Many electro-mechanical filters have been based on this principle using materials with low temperature coefficients of their elastic constant (e.g. the Invar steels) for the vibrating bodies and so shaping them that only single resonances occur in the waveband of interest. Above 1 MHz the resonant condition requires dimensions below 1 mm for most materials and, since this dimension needs to be controlled with the same precision as that required for the centre frequency of the filter, a considerable fabrication problem arises, though this can be alleviated to some extent by using the natural resonant frequency as a means of monitoring the relevant dimension.

Quartz was the first material in which the mechanical and electrical functions were combined [17] : the natural crystals provided a stable, reproducible raw material with, for specific cuts, near to zero temperature coefficients. Advantage was taken of its very low mechanical losses (high mechanical $Q = 10^4$ to 10^6) by making filters with sharply defined frequency boundaries, while its low piezoelectric coupling coefficient was compensated by combining crystals with inductor - capacitor networks when wide band width devices were required.

The far higher piezoelectric coefficients of ferroelectric materials led to the expectation that filters could be devised with a single body giving the entire filter characteristics since band width is proportional to k^2 (k = electromechanical coupling coefficient). This has indeed been the case for some wide tolerance applications but the lower mechanical Qs of ceramic bodies and the higher temperature coefficients of elastic

constants of both single crystals and ceramics has led to
limitations in high stability, close tolerance devices.

Now the following section [17] describes typical applications
using plates of piezoelectric ceramics (0.1 - 1 MHz):

Discs which are fully silvered on both faces and poled
normally to their electrodes have radial modes for their lowest
frequency resonances. The frequency factor, Nr, for the lowest
radial mode of PZT is about 1 KHzm so that discs of 10 to 2 mm
radius can cover the frequency range 100 to 500 KHz. The
fundamental resonance for the thickness mode occurs at a frequency
higher by a factor of approximately r/t, where r is the radius and
t the thickness of a disc.

If the reactance of a disc is plotted against frequency the
characteristic around resonance is as shown in Fig. 1.3.

Now equivalent circuit for the piezoelectric elements is
shown in Fig. 1.3.

Here R_1, L_1 and C_1 represent the mechanical losses, inertia
and elasticity and Co represents the electrical capacitance of the
element.

Now reactance of capacitance,

$$X_C = - \frac{1}{2\pi f r C_1}$$

Reactance of inductance, $X_L = 2\pi f r L_1$

At resonance, $2\pi f r L_1 = - \frac{1}{2\pi f r C_1}$

or, $\omega_o^2 = \frac{1}{L_1 C_1}$ \hfill 1.16

1.8 CLASSIFICATION OF FILTERS

According to Tetsuro Tanaka [18] among piezoelectric filters,
there are quartz filters, which have the longest history and

comparatively new filters such as mechanical filters, ceramic filters and SAW (Surface Acoustic Wave) filters. Although quartz filters are of the highest quality because they have a high Q and excellent frequency temperature characteristics, they are used only for narrow band filters because they have a small electromechanical coupling coefficient and they are expensive. $LaTiO_3$ and $LiNbO_3$ instead, can be used for wide band filters though they are also expensive. Quartz filters are mainly used for communication in a high frequency range.

M. Onoe [19] suggested that mechanical filters utilize a high Q and the excellent temperature characteristics of a constant elastic modulus alloy in combination with piezoelectric ceramics. They are of high quality but are not suitable structurally for very high frequency filters. They are rather suitable for low frequency filters, and they can offer even several hundred Hz, for example, by using the structure of a tuning fork.

According to Tanaka [18] ceramic filters are made solely of piezoelectric ceramics, whose Q value and temperature characteristics directly determine their quality. They are suitable for filters used in consumer electronics and are produced in greater number than all other filters because they have a considerably wide frequency range and because they are compact, strong and inexpensive.

SAW filters are the newest piezoelectric filters and utilize elastic waves which propagate on the surface of piezoelectric materials. Their frequency is determined by the dimensions of interdigital electrodes, whereas that of the other piezoelectric filters are determined by the shape and dimensions of the

material. Their quality is, therefore, determined both by the characteristics of the surface of piezoelectric materials and by the dimensions of electrodes. SAW filters are suitable principally for high frequency range and higher than GHz frequency ones are possible. They have a wide applicability ranging from a delay line to information processers.

1.9 PRINCIPLES OF PIEZOELECTRIC CERAMICS FOR MECHANICAL FILTERS

Piezoelectric ceramics are prepared for fabricating the electromechanical transducers used in the mechanical frequency filters that find application in long-haud communication systems. Also Mechanical frequency filters can offer additional advantages such as superior stability, smaller bulk and lower fabrication cost. Mechanical filters of uniformly high quality can be applied to the automatic mechanics, usually computer controlled, also for the fabrication of the filters and component elements, as well as for frequency tuning etc.

First filter developed was 50 KHz channel filter specifications [20] of the materials for that is listed in the Table 1.2.

Table 1.2 : Specifications of Piezo-ceramics for 50 KHz - filter

Permittivity	$\varepsilon/\varepsilon_o \approx 900 \pm 40$
Coupling coefficient	$k_{31} = 0.25 \pm 0.02$
Figure of merit	$\dfrac{\varepsilon}{\varepsilon_o} k_{31}^2 = 56$
Resonance Q	$Q \gg 600$
Temperature Coeff. of Permittivity	$Tc\varepsilon = \dfrac{\varepsilon(60^\circ C) - fr(20^\circ C)}{\varepsilon(20^\circ C)\ 40K} \leq 3000$ ppm/K
Temperature Coeff. of Frequency Constant	$TcF = \dfrac{fs(60^\circ C) - fs(20^\circ C)}{fs(20^\circ C).40K} = 80 \pm 50$ ppm/K
Aging offrequency Constantper time decade	$\Delta F \leq 0.1\%$

The resonance Q of the ceramics for the new signal filters

has to be at least three times higher. Also the temperature coefficient of the resonance Q, TcQ, must be very small. So for fabricating filter material we have to dope pure PZT with dopants like Fe, Cr, Mn or other acceptors which result high mechanical resonance Q. Also the high stability with respect to time of the frequency constant of ceramics doped with Cr or Mn makes them of interest for application in frequency filters. For resonators and filters temperature coefficient of frequency constant (TcF) values ranging between 0 and 80 ppm/K are required.

Principal properties of Mn doped Pb $(Zr_x Ti_{1-x})O_3$ ceramics for filters, as well as a portion of the phase diagram of these ceramics are discussed by H. Thomann and W. Wersing [20]. As with all lead zirconate titanate ceramics, the dielectric, piezoelectric and elastic properties and their temperature coefficients are closely related to the various ferroelectric phase transitions. The morphotropic tetragonal/rhombohedral phase boundary is of special interest because the permittivity and electromechanical coupling coefficient of the ceramics here reach their peak values. This is because spontaneous polarisation in the rhombohedral phase with its 8 possible directions can take on a more favorable orientation with respect to the applied electric field than is possible in the tetragonal phase with its 6 directions and also because the spontaneous strain in rhombohedral materials is less than in tetragonal, the rhombohedral phase is both electrically and elastically privileged during the polarization of such ceramics.

Ceramics doped with Cr, Mn and V give stabilizing effect. But for these, ceramics near the morphotropic phase boundary would

be generally unsuitable for filter application. Phas‑
stabilization is causally related to the stabilization of th‑
domain configuration. The stabilization of the domain
configuration in ceramics is directly indicated by their
hysteresis loops. Thus non polarised samples exhibit constricted
and polarized samples exhibit displaced hysteresis loops. This
effect is usually described by introducing an internal stabilizing
field E_i which is discussed earlier.

All symptoms of the stabilizing effect that is linearization
of the TcF, reduction of aging rate, appearance of an internal
field – appear to have the same physical origin.

Numerous models were discussed in the literature for the
purpose of explaining the stabilization are classifiable under
three basic concepts:

1. **Bulk Effect** [21]

Lattice defects of a dipole character (e.g. Mn" Ti – Vö)
assume orientation in the Lorentz field of spontaneous
polarisation and freeze the direction of polarisation.

2. **Domain Wall Effect** [21, 22]

Lattice defects diffuse to the domain walls, there by
reducing the domain wall energy and freezing the walls.

3. **Grain Boundary Effect** [10, 21]

Charged impurity atoms or vacancies accumulate at
nonsaturated domain configurations of neighboring grains and
freeze the direction of polarisation.

It is obvious that oxygen vacancies appear to be of critical
significance in all these models and stabilization can not be
attributed to a single effect in the case of all materials.

After treating the basic phenomena of significance in preparing filter ceramics based on lead zirconate titanate, we now discuss how the properties of filter ceramics can be improved by the combination of additions.

For filter ceramics the ternary system like $PbTiO_3-PbZrO_3-Pb(Mg_{1/3}Nb_{2/3})O_3$, and many other solid solutions like $Pb(Fe_{1/2}Nb_{1/2})O_3$, $Pb(Ni_{1/3}Nb_{2/3})O_3$, $Pb(Ni_{1/3}Sb_{2/3})O_3$ with $Pb(Zr,Ti)O_3$ are often additionally doped with a stabilizer such as Mn. The ternary $PbTiO_3-PbZrO_3-Pb(Mn_{1/3}Nb_{2/3})O_3$ system, reported for the first time by Wang [23] has composition with favorable planar electromechanical coupling factor kp and very high Qm and is recommended for filter ceramics. Also the temperature coefficient of resonance frequency (TcF) of the piezoelectric $Pb[(Zr_xTi_{1-x})_{0.95} (Mn_{1/3}Nb_{2/3})_{0.05}]O_3$ ceramics is investigated [23] by ways of Zr/Ti ratio, additive, sintering and poling temperatures. The morphotropic phase boundary (MPB) locates at x value near 0.51, where the planar electromechanical coupling factor (kp) reaches a maximum with TcF value of approximately 0 ppm/$^\circ$C. The ceramic composition exhibiting TcF values of 0 ppm/$^\circ$C is changed with processing conditions and be explained by the shift of the MPB compositions or the phase change.

Ceramics with optimally high permittivity and electromechanical coupling on the one hand, and high resonance Q and low aging rates on the other, are obtained by choosing an Mn/Nb ratio of $\approx$ 0.2. Ceramics with particularly favourable reproducibility with respect to the TcF are realized with zirconium mole fractions between 0.43 and 0.44.

Mechanical losses of filter ceramics should be as low as

possible and the mechanical resonance Q should be as high as possible in order to minimize the insertion loss.

To keep the insertion loss of narrow band signal filters sufficiently independent of the temperature, the temperature coefficient of the ceramics Q should be as low as possible ($|TCQ/Q| \leq 5$ ppm/K). Mechanical and electrical losses in soft piezoceramics mainly arise due to vibration of domain walls and their interaction with lattice point defects. Both Gerthsen, Härdtl and Schmidt and Arlt and Dederichs have developed models that describe the losses as a result of the damped motion of $90°$ domain walls. These models lead to the following relationship [24] between electrical ($\tan \delta$) and mechanical losses (1/Q)

$$1/Q = \tan \delta \frac{S_s^2 \cdot \varepsilon_{33}^T}{P_s^2 \cdot S_{11}^E} \cdot m \qquad 1.17$$

S_s = Spontaneous strain

P_s = Spontaneous polarisation

ε_{33}^T = Permittivity

S_{11}^E = Compliance

Mechanical losses in piezoelectric materials is related to electrical conductivity (σ) by the equation,

$$\tan \delta = \frac{\sigma}{\omega t} \qquad 1.18$$

The electrical conductivity of Mn doped ceramics ($10^{-10}-10^{-9}$ $1/\Omega m$) is far higher than that of ceramics doped with donors or complex oxides. Mn sometimes shows anomalously large dielectric losses due to inhomogeneous high conductivities ($10^{-5}-10^{-4}$ $1/\Omega m$) at grain boundaries. The resonance Q measured on such ceramics at about 100 KHz is only around 400.

CHAPTER 2
STATEMENT OF THE PROBLEM

One of the most important properties of piezoelectric resonators is its mechanical quality factor (Qm). Mechanical quality factor depends on the various impurities present in Lead Zirconate Titanate Ceramics. Based on literature survey we have chosen four dopants namely Nb_2O_5, MnO_2, Al_2O_3, Bi_2O_3.

Using design of experiments methodology an attempt has been made in present work to find out the optimum values of the different parameters (sintering time, sintering temperature, dopants concentration) needed for a tuner material.

CHAPTER 3

EXPERIMENTAL PROCEDURE

3.1 RAW MATERIALS:

The raw materials used for the preparation of PZT samples were as follows.

Table 3.1 : Details of Chemicals Used

	Chemicals	Purity	Manufacturer
1.	Lead Oxide (Yellow) (PbO)	99.9%	Aldrich chemical Company, Inc.
2.	Zirconia (ZrO_2)	99.9%	Magnesium Electr(Ltd (MEL) Grade,
3.	Titania (TiO_2)	99.9%	Aldrich chemical Company, Inc.
4.	Niobium Pentoxide (Nb_2O_5)	99.9%	Aldrich chemical Company, Inc.
5.	Manganese dioxide (MnO_2)	99.9%	Aldrich chemical Company, Inc.
6.	Bismuth Oxide (Bi_2O_3)	99.9%	Aldrich chemical Company, Inc.
7.	Alumina (Al_2O_3)	99.9%	Aldrich chemical Company, Inc.

3.2 PREPARATION OF ATMOSPHERE POWDER :

The composition of the atmosphere powder was selected as lead zirconate (PZ) (1 mole PbO : 1 mole ZrO_2) + 10 wt% PbO.

250 gms of batch material for the atmosphere powder was prepared by weighing PbO and ZrO_2 accurately. The batch material was put in a plastic jar. It was wet ball milled with Al_2O_3 balls for 6 hours. Triple distilled water was used as liquid media. It was dried in a breaker with constant stirring at $80^\circ C \pm 5^\circ C$. The dried powder was poured in a recrystallised alumina crucible and covered with a similar crucible. The whole assembly was

transferred to a pit furnace with silicon carbide heating elements. It was calcined at $860^{\circ}C$ for 1 hour. After taking out from the furnace the atmosphere powder which formed a compact was crushed to powder by agate mortar and pestle. A fast XRD scan of this powder confirmed the presence of lead zirconate, Lead Oxide, and zirconia phases only. The prepared powder was thus ready to be used as the atmosphere powder during the calcination and sintering of the PZT samples.

3.3 PREPARATION OF PZT COMPOSITIONS :

In the present investigation an attempt was made to obtain the optimum values of different variables in order to get maximum quality factor Qm and dielectric constant (before poling) of the sample. Effect of different variables like sintering time, sintering temperature, concentration (atom fraction) of dopants on dielectric constant and mechanical quality factor were studied.

3.4 RESPONSE SURFACE METHODOLOGY :

Response Surface Methodology (RSM) was used for this optimization study. This technique has been discussed elaborately by Kitttrell and Erjavee [25], Box et al. [26], Davies [27], Khuri and Cornell [28].

Let Y be the response of a chemical process dependent on the levels of K factors X_1, X_2,.... X_K which can be precisely measured and controlled. The model for the uth combination of factor levels is given by,

$$Y_u = \phi \left[X_{1u}, X_{2u}, \ldots \ldots, X_{Ku} \right] + \varepsilon_u$$
$$u = 1, 2, \ldots, N$$

where, N is the number of experiments

ϕ is the functional relationship, and

ε is the error involved.

A geometrical portrait of the response function in the factor space is called a response surface. The experimental region R, is a bounded subspace of the whole factor space. The experimental region is bounded because of the practical limitations. The response surface methodology locates a point $(X_1^o, \; X_2^o, \; ...., \; X_K^o)$ within the experimental region R, at which Y is an extremum [29.30.31]. The traditional one factor at a time method, where the experiments are conducted holding all the other factors constant often fails to locate the true optimum.

The response surface methodology cuts down the experimental effort by making use of experimental designs which permit the experimenter to assess the strength of the interactions between the factors while varying them simultaneously [30].

RSM consists of several steps.

1. The first step is to design a set of experiments and conduct them to get reliable estimates of the parameters. When the number of factors is small, factorial design can be used. On the other hand, fractional factorial designs are used when the number of factors are large. The details of factorial and fractional factorial designs are discussed by Box et al. [26] and Rao and Iyengar [32].

2. A suitable mathematical model is proposed to fit for the experimental data and then test for model adequacy through Lack-of-fit F-tests [33].

3. To find out the optimum conditions of the independent

variables which will produce the maximum (or minimum) value of the response. At a point which is remote from the optimum, there is a little curvature in the true response surface and first order models will be satisfactory to describe the response surface. In the vicinity of the optimum, however, higher order models will be required due to the presence of curvature in the response surface.

RSM is sequential in nature. Some experiments are carried out, valuable information is gathered and the next stage is designed for getting better values of the response. Generally the method of steepest ascent (or descent) is applied for moving sequentially along the direction of maximum (or minimum) increase (or decrease) in response.

3.3.2   VARIABLES IDENTIFICATION AND THEIR LEVELS :

Important variables which influence the dielectric constant and mechanical quality factor are sintering time, sintering temperature, atom fraction of various dopants. The dopants selected in the study are Nb_2O_5, MnO_2, Al_2O_3 and Bi_2O_3. After knowing the important variables influencing the process, a base level had to be chosen within the experimental region. The base levels of the factors were chosen on the basis of an a priori knowledge. Further the variation interval for each factor had to be chosen. The variation interval of a factor when added or substrated from the base levels gives the upper or the lower level of the factor respectively.

To simplify the recording of the conditions of an experiment, and the processing of the experimental data the values of the

factors were coded as follows:

$$X_i = \frac{\overline{X}_i - \overline{X}_{i0}}{\nu_i} \qquad i = 1, 2, \ldots, K$$

where X_i is the coded value of the i-th factor

$\overline{X}_i$ is the natural value of the i-th factor,

$\overline{X}_{i0}$ is the natural value of the base level of the i-th factor, and ν_i is the variation interval of the i-th factor.

Conventionally, the coded value of upper level corresponds to +1, the lower level to -1 and the base level to 0. The upper, lower and base levels of the variables in this first stage of design are given in Table 3.2.

The following dependent variables (responses) were considered to be important for optimization.

a.   dielectric constant (before poling)

b.   mechanical quality factor.

Table 3.2 : First Order Response Surface Strategy (First Move)

LEVEL OF FACTORS

Factor	Code	Base level	Lower Level (-)	Higher Level (+)
Sintering time (hrs)	X_1	3	2	4
Sintering Temp. ($^\circ$C)	X_2	1240	1220	1260
Nb_2O_5 (atom fraction)	X_3	0.045	0.01	0.08
MnO_2 (atom fraction)	X_4	0.025	0.01	0.04
Al_2O_3 (atom fraction)	X_5	0.06	0	0.12
Bi_2O_3 (atom fraction)	X_6	0.01	0	0.02

3.3.3   SELECTION OF EXPERIMENTAL DESIGN :

Since there are six variables, a 2^{6-2} fractional factorial

design around the base levels was employed. The design matrix is shown in Table 4.1. The basis for choosing $X_5 = X_1 X_3$ and $X_6 = X_1 X_4$ as these combinations are expected to have minimum interactions. Experiments were carried out in a randomized sequence to avoid bias, on the part of experimenter. The values of all the responses (dielectric constant, mechanical quality factor) for the first move of experiments (runs numbered 1 to 16) as planned in the design matrix are given in Table 4.1. Experiment No. 4 was repeated three times so as to obtain an estimate of the error.

3.4 SAMPLE PREPARATION:

PZT compositions with four dopants were prepared by standard ceramic processing route. Dopants were Nb_2O_5, MnO_2, Bi_2O_3, Al_2O_3. The morphotropic phase boundary in $Pb(Zr_x Ti_{1-x})O_3$ lies at $X \simeq 0.535$. Eight different compositions were prepared having this value of X but part of ZrO_2, TiO_2 and PbO were replaced by dopants so that composition can be represented by

$$Pb_{1-m}Bi_m\left[\left(Zr_{0.535}Ti_{0.465}\right)_{1-y-z-\omega}Al_y Mn_z Nb_\omega\right]O_3$$
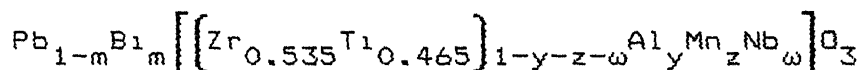
Eight sets of samples of following composition were prepared.

(i) $Pb\left[\left(Zr_{0.535} Ti_{0.465}\right)_{0.79} Al_{0.12} Mn_{0.01} Nb_{0.08}\right]O_3$

(ii) $Pb\left[\left(Zr_{0.535} Ti_{0.465}\right)_{0.98} Mn_{0.01} Nb_{0.01}\right]O_3$

(iii) $Pb\left[\left(Zr_{0.535} Ti_{0.465}\right)_{0.85} Al_{0.12} Mn_{0.04} Nb_{0.01}\right]O_3$

(iv) $Pb\left[\left(Zr_{0.535} Ti_{0.465}\right)_{0.88} Mn_{0.04} Nb_{0.08}\right]O_3$

(v) $Pb_{0.98} Bi_{0.02}\left[\left(Zr_{0.535} Ti_{0.465}\right)_{0.86} Al_{0.12} Mn_{0.01} Nb_{0.01}\right]O_3$

(vi) $Pb_{0.98} Bi_{0.02} \left[(Zr_{0.535} Ti_{0.465})_{0.91} Mn_{0.01} Nb_{0.08} \right] O_3$

(vii) $Pb_{0.98} Bi_{0.02} \left[(Zr_{0.535} Ti_{0.465})_{0.95} Mn_{0.04} Nb_{0.01} \right] O_3$

(viii) $Pb_{0.98} Bi_{0.02} \left[(Zr_{0.535} Ti_{0.465})_{0.76} Al_{0.12} Mn_{0.04} Nb_{0.08} \right] O_3$

Each of these above compositions were sintered at two different temperatures (i) $1220^{\circ}C$ and (ii) $1260^{\circ}C$. The sintering time was 2 hrs or 4 hrs as per the design matrix (Table 4.1). A total of 16 distinct combination of all the factors plus three repeats of combination No. 4 were used giving a total of 19 experiments as per Table 4.1. 5 wt% excess PbO were added for those compositions which were sintered at high temperature $1260^{\circ}C$.

20 gms of batch materials for each of 16 compositions were prepared. Individual oxide component was weighed accurately. Then each batch were ball-milled for 10 hrs and dried in exactly same way as described in section3.2. Dried powder was crushed in mortar pestle and then loosely poured in the recrystallised alumina crucible. Atmosphere powder was taken in a platinum crucible. It was placed over the loose powder. The system was covered with similar alumina crucible. The total assembly is shown in Fig. 3.1(a). It was then put in the pit furnace. The calcination was done at $900^{\circ}C$ for 4 hours for all the batches.

The calcined aggregate of each set was crushed into powder in agate mortar and pestle. The powder was then sieved through a 100 mesh sieve and mixed with PVA (Poly vinyl alcohol) solution (4% by wt) to yield 1 wt% PVA of the powders. Then water was added to make a slurry. After thorough mixing it was dried at $60^{\circ}C \pm 5^{\circ}C$ in an oven. The dried powder formed a lump which was crushed again

in mortar pestle and passed through 100 mesh screen (ASTM). Pellets were made with fixed amount of powder and well compacted using 5 tons pressure for 1 minute in a die of 12mm diameter. Pellets of 5 mm thickness were formed.

The prepared pellets were sintered with atmosphere powder according to sintering schedule given in the Table 4.1. The heating rate was 3°C/min and the cooling rate was 4°C/min. The entire sintering assembly is shown in Fig.3.1(b). Before sintering pellets were held at 600°C for 4 hours to drive out adsorbed water and binder respectively. The weight of the pellets were taken after cooling down to room temperature. This is the weight of pellet before sintering. Finally the pellets were sintered and again weight of the pellets were taken after cooling down to room temperature. This is the weight of pellet after sintering. These two weights were required for finding out the amount of Pb - loss. These pellets were used for all further studies.

3.5   XRD ANALYSIS:

XRD analysis of sintered pellet for 16 different compositions were made by a REICH SEIFERT ISO DEBYEFLEY 2002 DIFRACTOMETER. CuK_{α} (λ = 1.5405 Å) radiation was used.

The X-ray diffraction plots of the sample were taken in the 2θ range of 20° to 70° with the chart speed 3 cm/min and scanning speed 3°/min and full scale intensity 10K counts/min. Also slow scanning were taken in the 2θ range of $30^{\circ}-33^{\circ}$, $37^{\circ}-39^{\circ}$, $43^{\circ}-46^{\circ}$ with the following operating conditions.
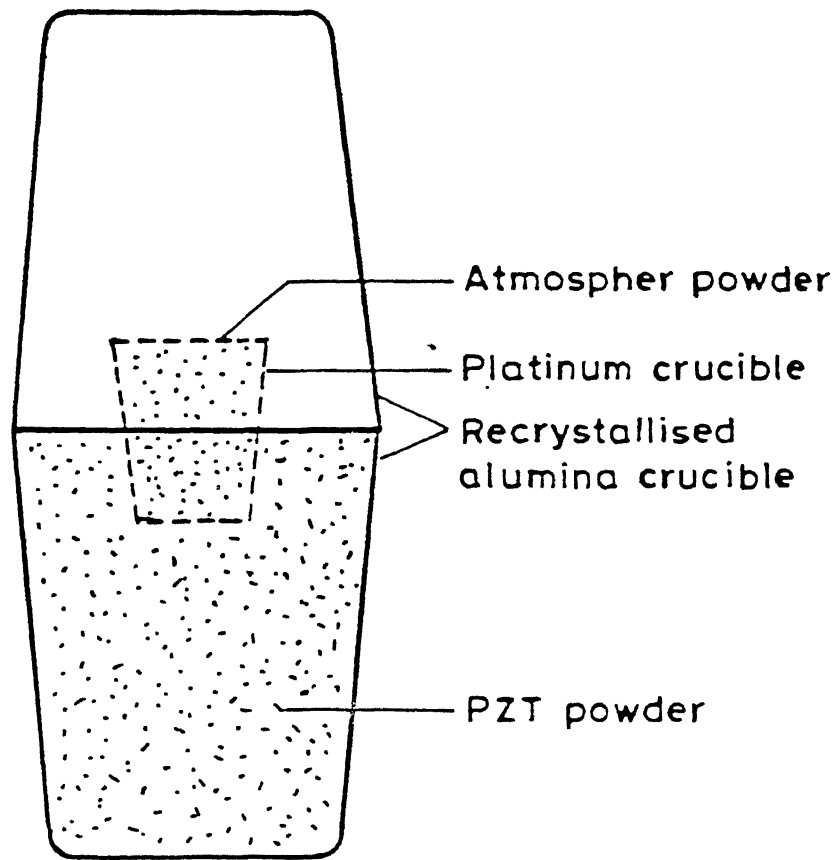
Fig. 3.1(a) Schematic diagrdm of crucible arrange-
ment during calcination.
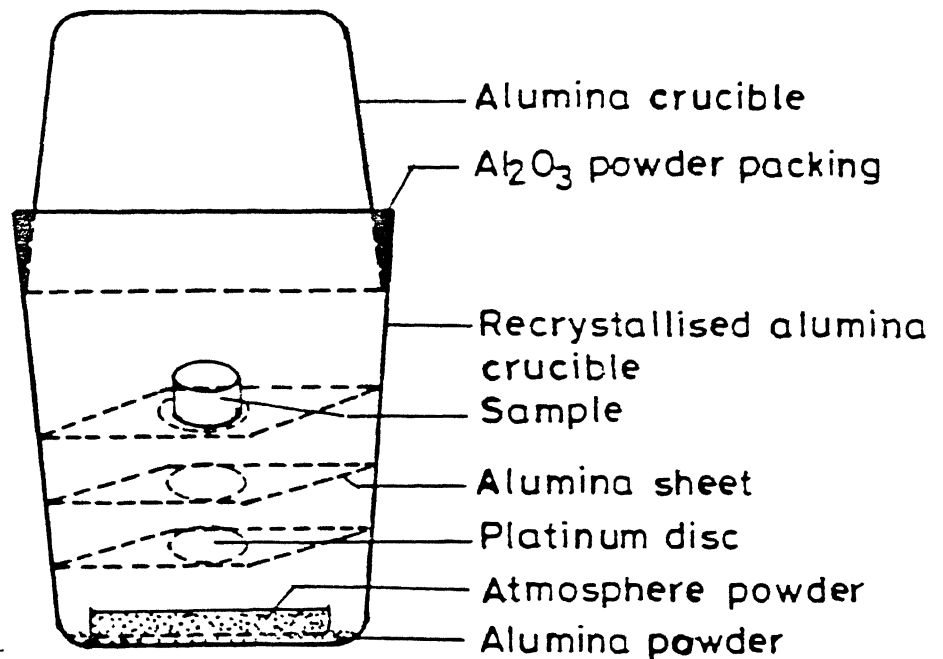
Fig. 3.1(b) Schematic diagram of crucible arrange-
ment during sintering.

Operating Conditions of Diffractometer during X-ray Diffraction

Current, Voltage   —   20mA, 30KV

Time constant   —   10 seconds

Beam slit width   —   1.5 mm

Detector slit width   —   0.3 mm

Scanning speed (2θ)   —   0.6°/min

Chart speed   —   0.6 cm/min

Full Scale Intensity   —   10 K counts/minute,

                                20 K counts/minute.

From the diffraction pattern (2θ vs Intensity) the phases present were identified from the peak positions. The peak positions were compared with standard X-ray data files.

3.6   MEASUREMENT OF SINTERED DENSITY :

The sintered density of the prepared samples were measured by water displacement method. The initial dry weight (w_1) of the samp was taken using a ACFOSET ER-120A ELECTRONIC BALANCE. The sample was then immersed in a water and kept under vacuum for 1 hour in order to allow water to enter into the pores of the sample. Then weight of sample suspended in water (w_2) was taken. The sample w. then taken out and dabbed with tissue paper and cotton. The weight of the sample, saturated with water was finally taken. The sintered density was calculated from the following relation.

$$\text{SINTERED DENSITY} = \frac{w_1}{w_1 - w_2}$$

3.7   SCANNING ELECTRON MICROSCOPY :

Fracture surface of the PZT samples were observed using JSM – 840A Scanning Microscope, JEOL.

The sample was broken before putting it in the microscope and

was cleaned thoroughly using ultrasonic vibrator. Then it was mounted on an aluminium stub using a silver paint. For each sample exposed surface was coated with gold-paladium in a dc sputtering unit (Anatech Ltd.) an operating voltage 5 K.V., plasma atomic discharge current 10 mA, and for 5-6 minutes.

3.8 MEASUREMENT OF PIEZOELECTRIC PROPERTIES :

3.8.1 d_{33} measurement :

Disc shaped samples of 1 mm thickness were cut using a diamond rimmed circular blade, polished with 3(0), 4/0 emery paper and cleaned with actone in an ultrasonic bath. The discs were then coated by silver paint on both surfaces except the edges. Using a multimeter the continuity of each surface and the discontinuity between the two surfaces was checked. A strong electric field was then applied to the disc placed tightly between a brass cathode and an aluminium anode using a fixture schematically shown in Fig.3.2.

To avoid dielectric breakdown, the whole fixture was put in a beaker containing silicone oil. The beaker was heated and temperature of the oil was maintained between 110 to 120°C. The poling field was along the thickness. The following conditions were used

    Applied field =   3.5 KV/mm

    Temperature   =   110 - 120°C

    Time   =   30 mins.

When the temperature reached about 100°C, the electric field was switched on and after holding at a temperature around 110°C to 120°C for 30 minutes, the sample was cooled by switching off the
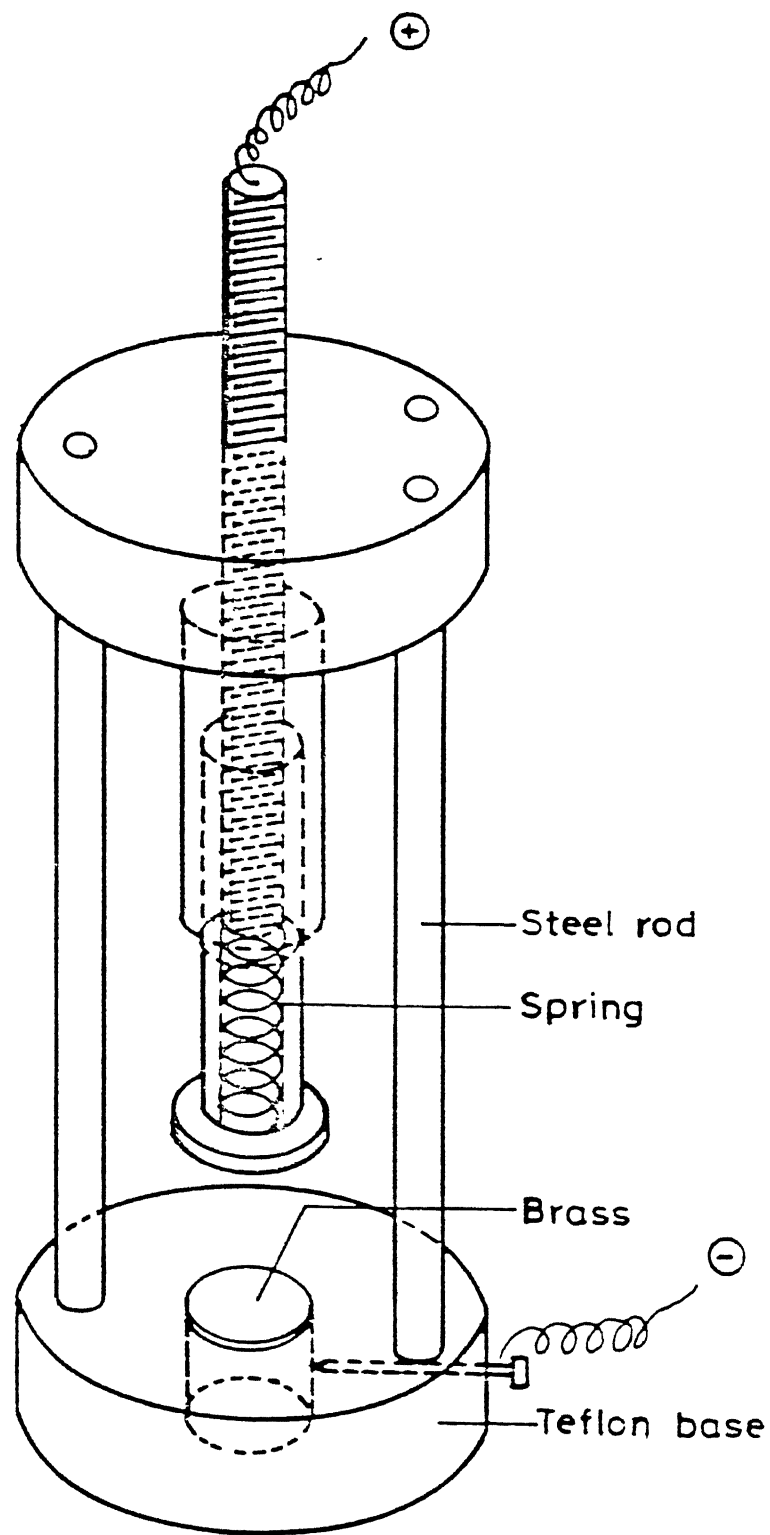
Fig. 3.2 Schematic diagram of poling fixture.

heater with the field on. When the temperature reached the room value, the field was switched off. Cooling to room temperature took about 7-8 minutes. The discs were then taken out of the poling fixture and silicone oil was removed by gently rubbing with cotton, care being taken not to remove the Ag coating. The poled samples were then kept for 24 hours after which d_{33} measurements were made. A channel products, Belincourt d_{33} meter was used for d_{33} measurement, at 25 Hz.

3.8.2   Measurement of Resonance and Antiresonance Frequencies

Measurement Techniques

Two types of techniques can be used:

(i)   Static method

(ii) Dynamic method

Piezoelectric constants may be measured by the techniques of static method with reasonable accuracy but the precision is inferior to that obtained with dynamic method. Hence the discussion is restricted to later method only.

Elastic bodies show numerous resonances. But the most pronounced are those where the body can just accommodate one half wavelength of a standing wave. Piezoelectric effect is used to excite such elastic wave and to observe interaction of the mechanical resonance with electric field behaviour.

Resonance Method

This is a simple dynamic method for evaluating piezoelectric constants by measuring the resonant (fr) and antiresonant (fa) frequencies corresponding to a longitudinal mode by means of a simple electric circuit as shown in the Fig.3.3.
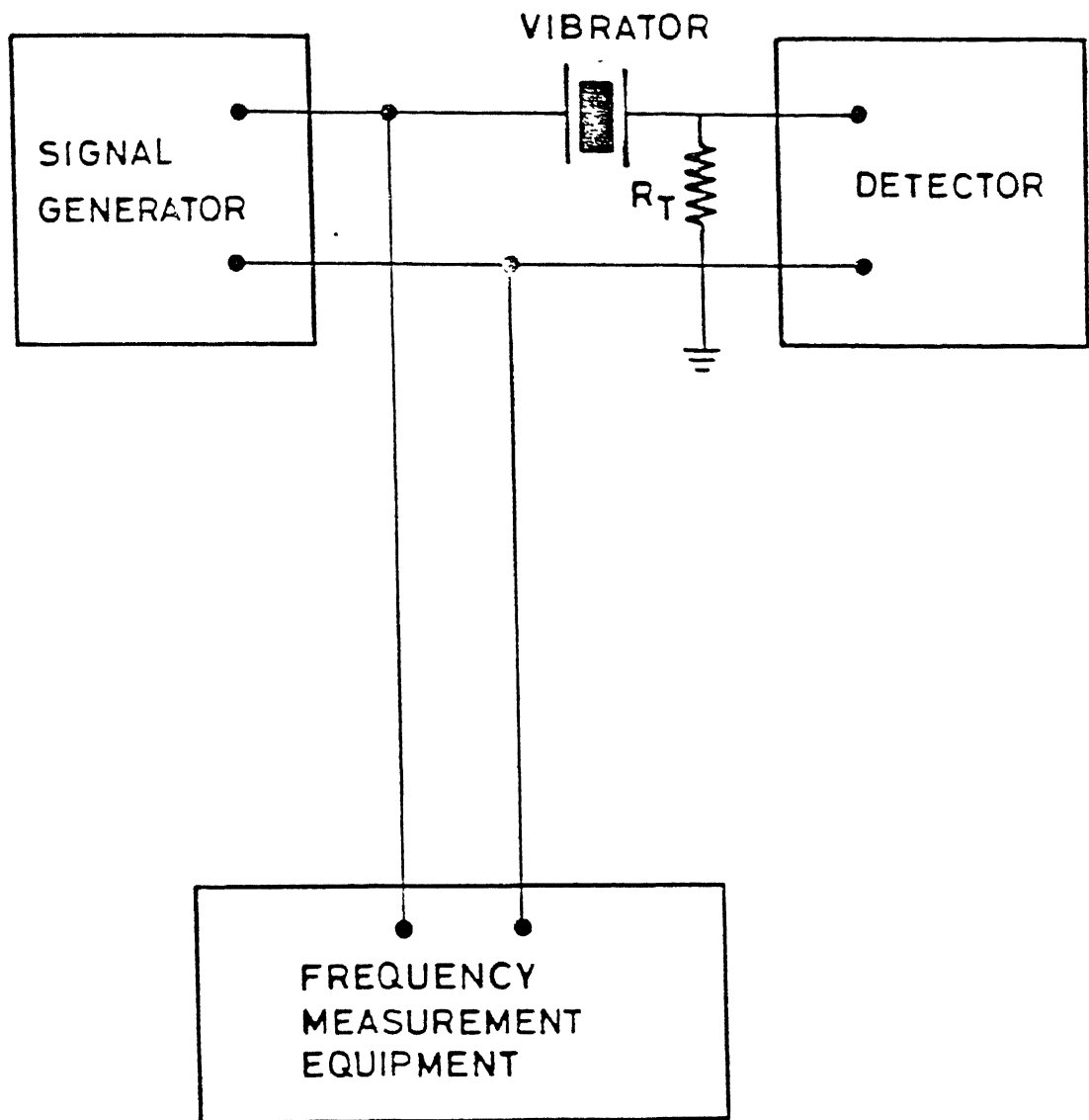
Fig. 3.3 Transmission net work for determination of f_r and f_a of piezoelectric ceramic vibrator.

When the piezoelectric material is put in the circuit, the electric field sets up vibration in the material through direct piezoelectric effect. The commonly encountered modes of motion of bars, plates and disks excited piezoelectrically by electric field are

i.   Length extensional mode

ii.   Overtone contour-shear mode

iii. Contour extensional mode

iv.   Contour mode

v.   Contour extensional mode (disk)

The first two modes of motion are for narrow bars, third and forth correspond to square plate and the last mode of motion is for disk.

The periodic vibration of the crystal causes periodic piezoelectric changes on the electrode through converse effects. The properties of any mode of a lightly damped mechanical vibrating system (excited piezoelectrically) can be represented near resonance by an equivalent electric circuit as shown in Fig.1.3. which consist of a capacitance C_1, inductance L_1, and resistance R_1, in series, shunted by a second capacitance C_o in parallel. These are the fundamental parameters of the piezoelectric vibrator. The parameters are independent of frequency if the vibrator has no other mode of motion near resonance.

The equivalent series resistance and reactance of the $R_1 L_1 C_1 C_o$ circuit is given by

$$R_s = \frac{R_1}{\left[1 - WC_oX\right]^2 + W^2C_o^2R_1^2}$$

$$X_s = \frac{X - WC_o\left[R_1^2 + X^2\right]}{\left[1 - WC_oX\right]^2 + W^2C_o^2R_1^2}$$

where $X = WL_1 - \frac{1}{WC_1}$, reactance of the R_1, L_1, C_1 branch in the series. The resonance frequencies are obtained by setting $X_s = 0$. At resonance R is nearly zero.

Solving this series resonance, fs, is given by

$$f_s = \frac{1}{2\pi(L_1C_1)^{1/2}}$$

Similarly parallel resonance frequency can be obtained as

$$f_p = \frac{1}{2\pi}\left[\frac{C_o + C_1}{L_1C_oC_1}\right]^{1/2}$$

Variation of series reactance, X_s, with frequency is shown in Fig. 1.3. Piezoelectric properties are measured using their resonant fr (minimum impedance) and antiresonance fa (maximum impedance) frequencies. Complete scheme of measurements are given in Appendix 1.

Here the measurements are restricted to disk shaped samples. Only fr and fa are measured by using 4194A IMPEDANCE/GAIN PHASE ANALYSER (HEWLETT-PACKARD).

Planar coupling coefficient kp, is obtained from the fr and fa values of the thin disk with faces perpendicular to z-axis as follows:

$$\frac{k_p^2}{1-k_p^2} = \frac{(1 - \sigma^E)J_1[\eta_1(1 + \frac{\Delta f}{fr})] - \eta_1(1 + \frac{\Delta f}{fr})J_o[\eta_1(1 + \frac{\Delta f}{fr})]}{(1-\sigma^E)J_1[\eta_1(1 + \frac{\Delta f}{fr})]}$$

where J_o = Bessel function of first kind and zero order

J_1 = Bessel function of first kind and first order

η_1 = Lowest positive root of $(1+\sigma^E)J_1 = \eta J_o(\eta)$

For σ^E = 0.3 (poisson ratio), η = 2.05.

The relationship is plotted in Fig. 3.4 where kp is shown as a function of $\Delta f/fr$ [4]. The value of kp is read directly from this plot.

k_{33} and k_{31} are calculated as follows:

$$k_{33}^2 = \frac{\pi}{2} \frac{fr}{fa} \tan\left(\frac{\pi}{2} \frac{\Delta f}{fa}\right)$$

$$k_{31}^2 = \left(\frac{1-\sigma^E}{2}\right) k_p^2$$

d_{33} was measured by using the CHANNEL PRODUCTS, MODEL CPDT 3300 BERLINCOURT PIEZO d_{33} METER,

d_{31} is calculated as follows:

$$d_{31} = K_{31} \left[\varepsilon_{33}^T \; S_{11}^E\right]^{1/2} \text{ coulombs/Newton}$$

where

$$\frac{1}{S_{11}^E} = \frac{\pi^2 d^2 fr^2 \left(1 - \sigma^{E^2}\right) \rho}{\eta_1^2}$$

d = diameter of disk

ρ = density of disk

η_1 = 2.05

σ^E = 0.3 (usually between 0.29 to 0.33)

ε_{33}^T = Free dielectric constant, obtained as shown later

g_{33} is given by

$$g_{33} = \frac{d_{33}}{\varepsilon_{33}^T} \frac{\text{Volt meter}}{\text{Newton}}$$

K_{33}^S (relative clamped dielectric constant, longitudinal) is calculated as:

$$K_{33}^S = \frac{C \times T}{A \times 8.854 \times 10^{-12}}$$

C = capacitances in Farad
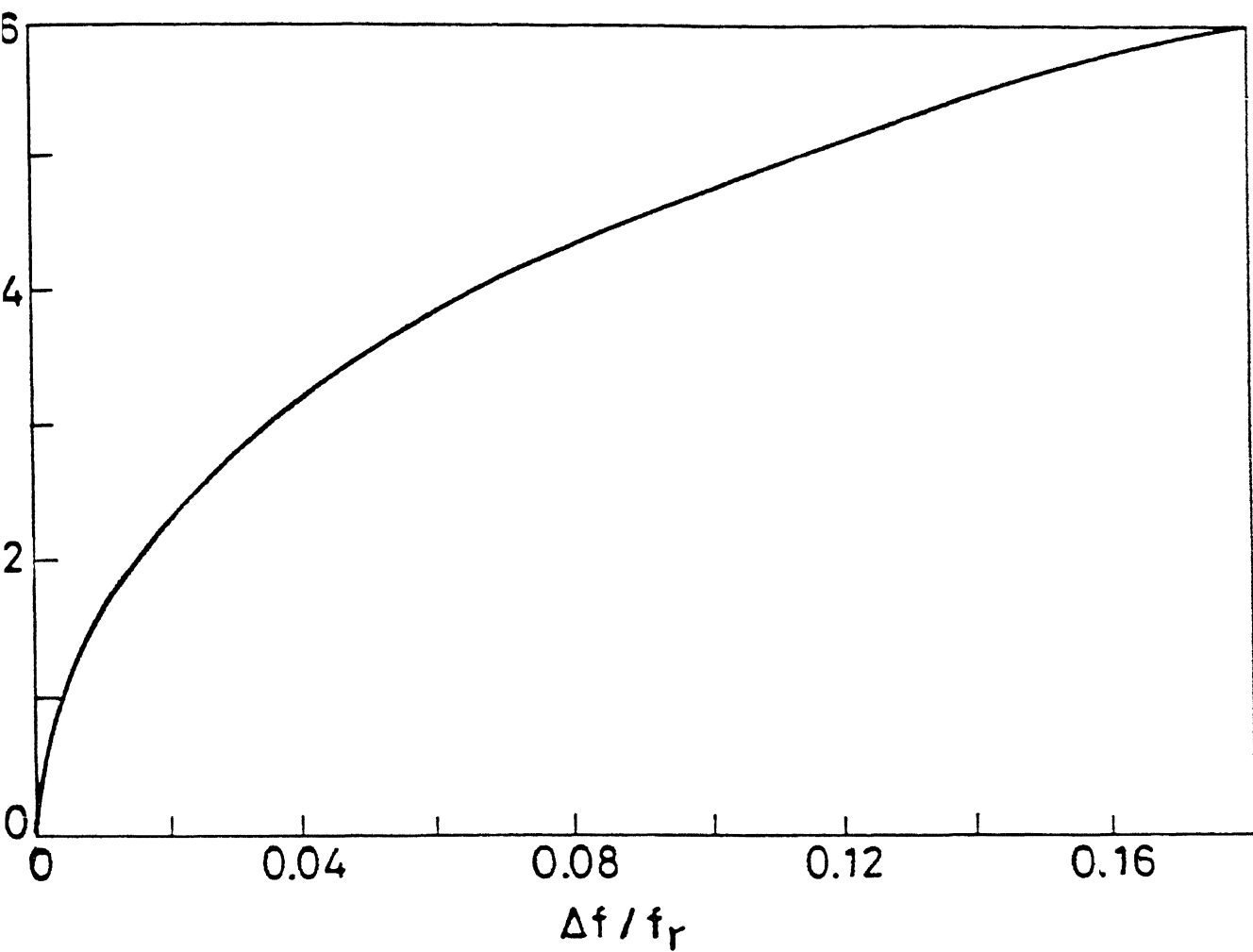
Fig. 3.4 Planar coupling factor of thin disk.

t = thickness in m

A = Area in m^2

ε_{33}^T = K_{33}^T × 8.854 × 10^{-12} Farad/meter

K_{33}^T (relative free dielectric constant) is calculated from K_{33}^S by

$$K_{33}^T = \frac{K_{33}^S}{1 - k_p^2}$$

Qm can be determined by means of the piezoelectric resonance with a radial fundamental mode. Thus value of Qm is obtained by means of the relation given below,

$$\frac{1}{Qm} = 2\pi frCR \left\{ 1 - \left[\frac{fr}{fa}\right]^2 \right\}$$

where

fr = resonance frequency

fa = antiresonance frequency

R = resistance at resonance

C = Capacitance at 1KHz.

CHAPTER 4

RESULTS AND DISCUSSION

4.1 DENSITY AND Pb LOSS :

Theoretical density and % Pb loss of the 16 sets of PZT compositions are shown in table 4.6.

The results are plotted as a function of (a) different dopant concentration and (b) sintering temperature in Fig.4.1. Here all the data points are used. This is a valid procedure in the analysis of data from the designed experiments.

With the variation of doping concentration density varies. It is observed that % theoretical density reaches higher values when doping with 0.08 atom fraction of Nb_2O_5 in all but one experiment. Also with zero atom fraction of Al_2O_3, the density tends to reach maximum values. The effect of other dopants on densities is not discernible. Increasing the sintering temperature from $1220^\circ C$ to $1260^\circ C$ also does not result in any increase in density.

The effect of dopant on the sintered density is through their effect on the rate of grain growth. If the grain growth is restricted then high density can be achieved because the diffusion distance for vacancies from a pore in the centre of a grain to the grain boundary is less. Thus the aluminium substitutes at B sites and creates an oxygen vacancy while Nb also substitutes at B site but creates Pb vacancies. Each is associated with its corresponding charge vacancies and seggregate to grain boundary making grain growth difficult [15].

When both Nb and Al are doped together, they associate with

each other rather than with vacancies and so do not seggregate to grain boundary and do not affect grain growth. Individually Nb is found to be most effective and Al less effective while when both are present no significant effect is observed. This is consistent with our observation that highest densities are obtained when only Nb is present and the density is reduced when both are added together.

The data for Pb loss has been similarly plotted in Fig.4.1.

It is found that % Pb loss increases with increase in sintering temperature from $1220^\circ C$ to $1260^\circ C$ irrespective of the composition. Also variation of % Pb loss is significant with the variation of atom fraction of Al_2O_3 from 0 to 0.12. There is also Pb gain for some composition.

The effect of a trivalent dopant on Pb loss or gain has been discussed by Wu et al. [34]. The general equation for a trivalent dopant with some excess PbO (AO) is represented by the following equation,

For trivalent doping:

$$ABO_3 + XM_2O_3 + 2pxAO \rightarrow A_{(1+2pX-3qx-(3r/2)x)}$$
$$M_{2(q+r)x} \square_{qx} [BM_{2px} \square_{(r/2)x}]O_3 + 5px + (\frac{3r}{2})x \square_{px}$$
$$+ (3q + \frac{3r}{2}) XAO \uparrow$$
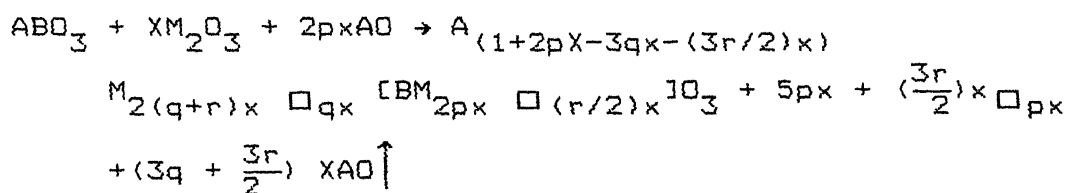
For the specific case of M^{3+} on the A site with A-site vacancy we have

$$ABO_3 + XM_2O_3 \rightarrow [A_{(1-3X)} M_{2x} \square_x] [B]O_3 + 3 XAO \uparrow \text{ loss}$$
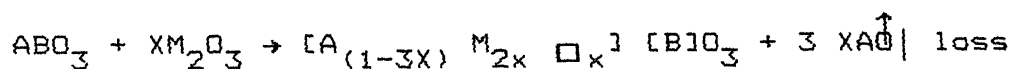
For M^{3+} on A site with B site vacancy only

$$ABO_3 + XM_2O_3 \rightarrow A_{(1-1.5X)} M_{2x}] [B \square_{(x/2)} O_{1+1.5x} + 1.5 XAO \uparrow \text{ loss}$$
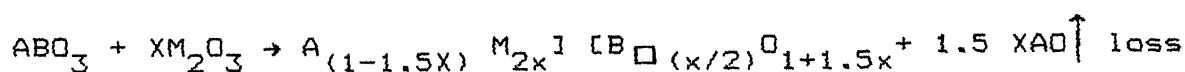
For M^{+3} on B site with O vacancy
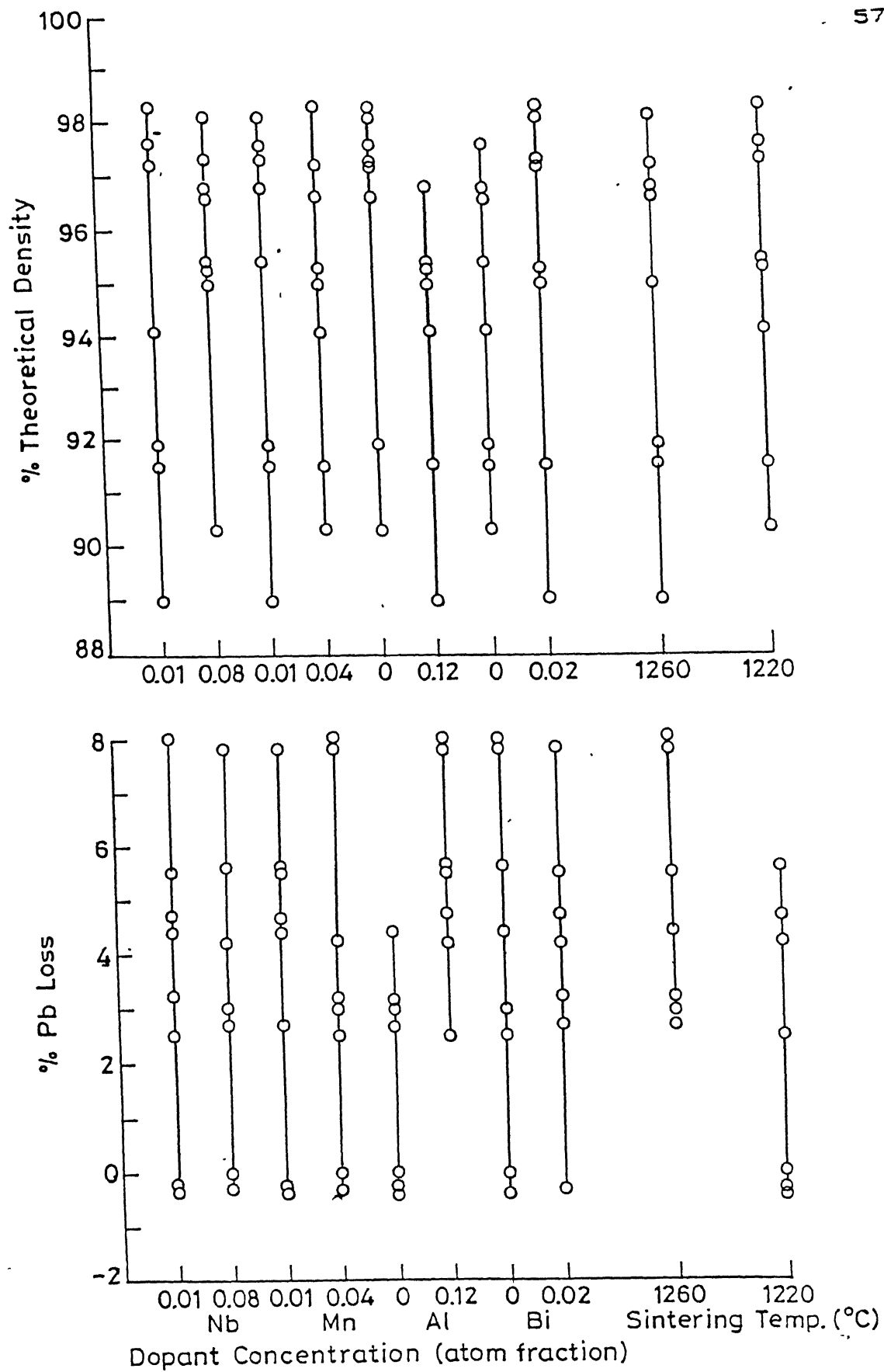
FIG. 4.1   Variation of % theoretical density and % Pb loss with different dopant concentrations and sintering temperatures

$$ABO_3 + XM_2O_3 + 2XAO \text{ (gain)} \rightarrow [A_{1+2x}][BM_{2x}]O_{3+5x} \square_{x/2}$$
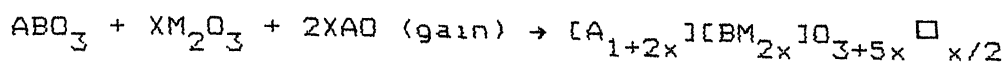
Thus depending on the site to which the dopant goes and the site at which vacancy is created one can have either a loss or a gain in the weight. In general if the dopant M^{3+} goes to B site then an equal number of Pb atoms come to the newly create A site leading to an increasing weight. However even though it is known that Al^{+3} goes to the B site, we find that there is a loss of weight instead of an increase in weight. Obviously the effect of other dopants dominate.

4.2 SCANNING ELECTRON MICROGRAPHS (SEM) ANALYSIS :

Microstructure of six sets of samples are shown here (Fig. 4.2.1, 4.2.2., 4.2.3, 4.2.4). From the microstructures it is clear that samples (R1, R2, R13, R14) which are poled of smaller in grain size and samples (R9, R12) that cannot be poled are of larger in grain size.

The large grain size results in-excessive strain during poling causing the samples to break. Most of the samples (all except one) contain low amounts of Nb and also high amount of Mn. Apparently there is complex interaction between the various dopants which control the grain growth. The breakage of sample during poling appears to be solely because of large grain sizes.

4.3 XRD ANALYSIS

The obtained results (Table 4.6) indicate that the tetragonality increases on increasing sintering temperature for all compositions except one (R3, R5). Some representative X-ray scans are shown in Fig. 4.3 and 4.4. Appreciable shifts in the peak positions are also observed for samples of different
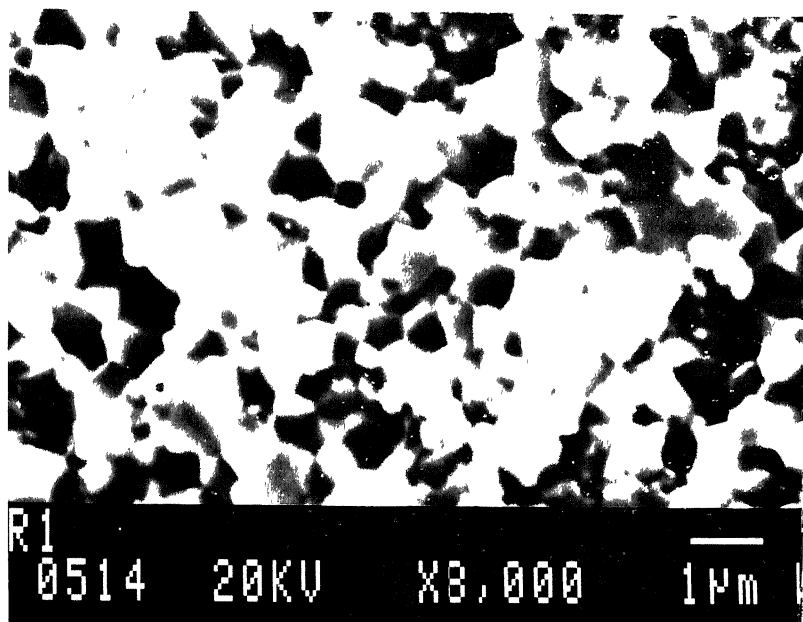
(a)
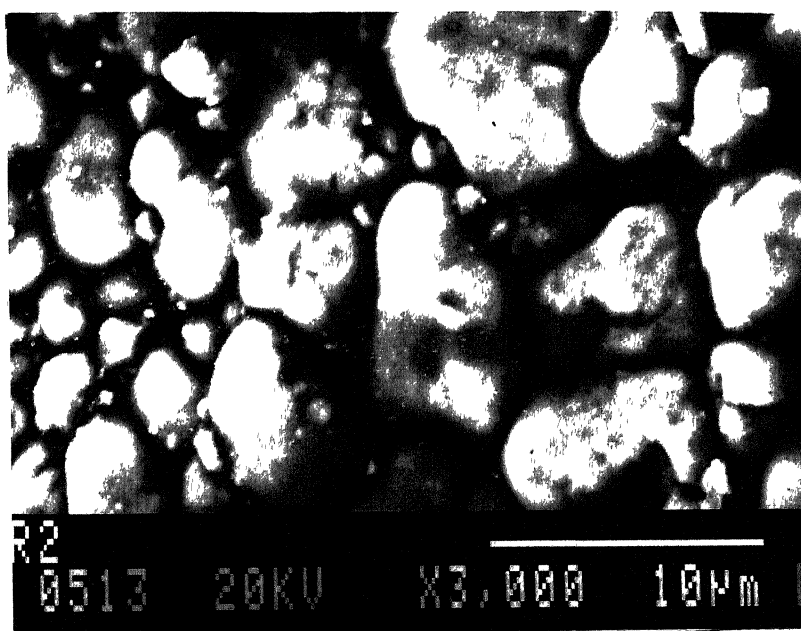
(b)

FIG. 4.2.1   Microstructure   of   sample

(a)   R1 $(Nb_{0.08}Mn_{0.01}Al_{0.12})$

(b)   R2 $(Nb_{0.01}Mn_{0.01})$
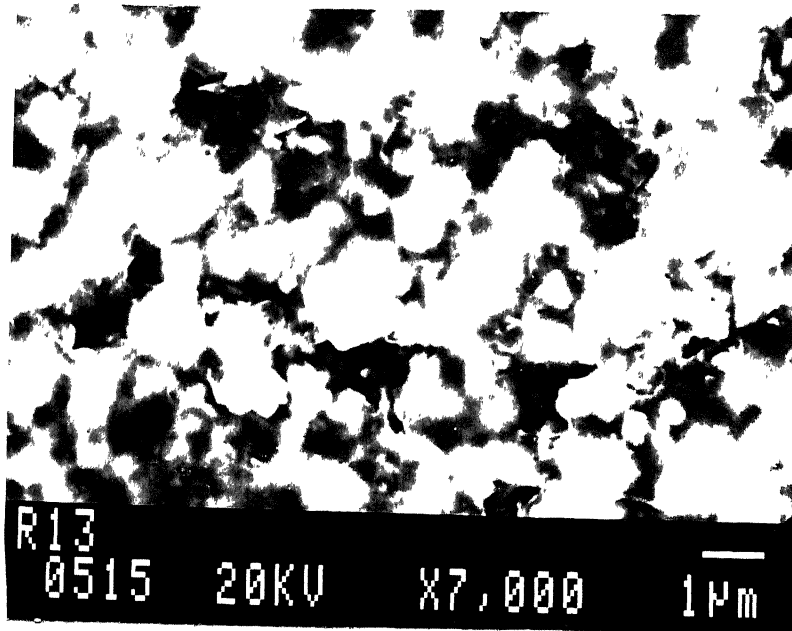
(a)

(b)

FIG. 4.2.2   Microstructure of sample

(a)   R13 $(Nb_{0.08}Mn_{0.04})$

(b) . R14 $(Nb_{0.08}Mn_{0.04}Al_{0.12}Bi_{0.02})$
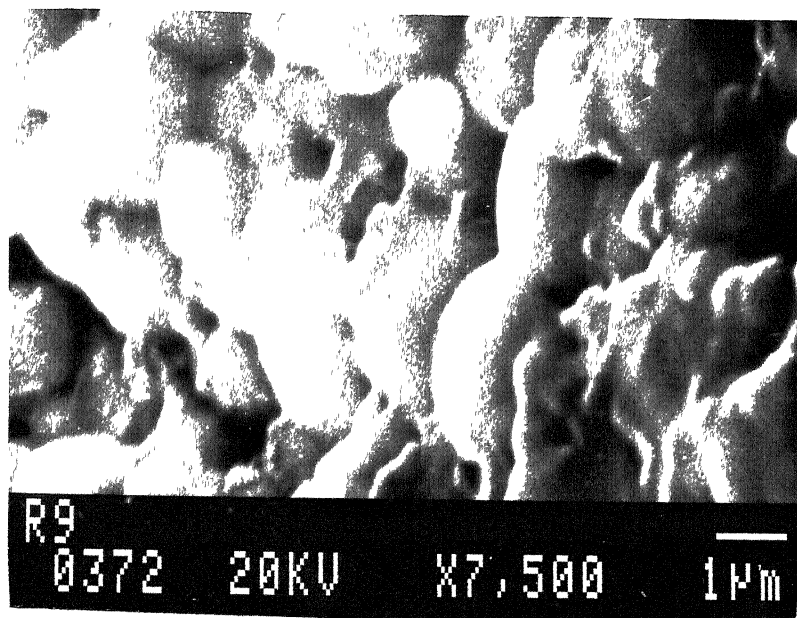
(a)
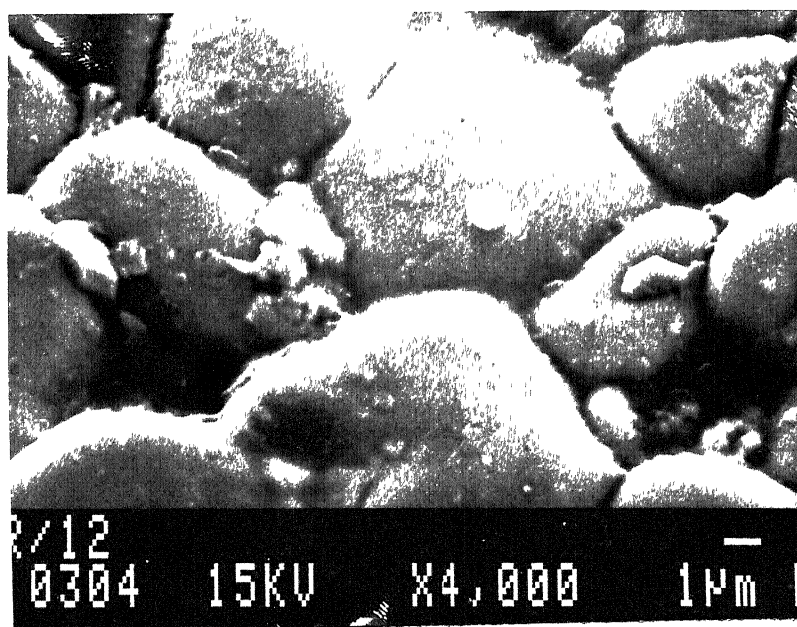
(b)

FIG. 4.2.3   Microstructure   of   sample

(a)   R9 $(Nb_{0.01}Mn_{0.04}Al_{0.12})$

(b)   R12 $(Nb_{0.01}Mn_{0.04}Bl_{0.02})$
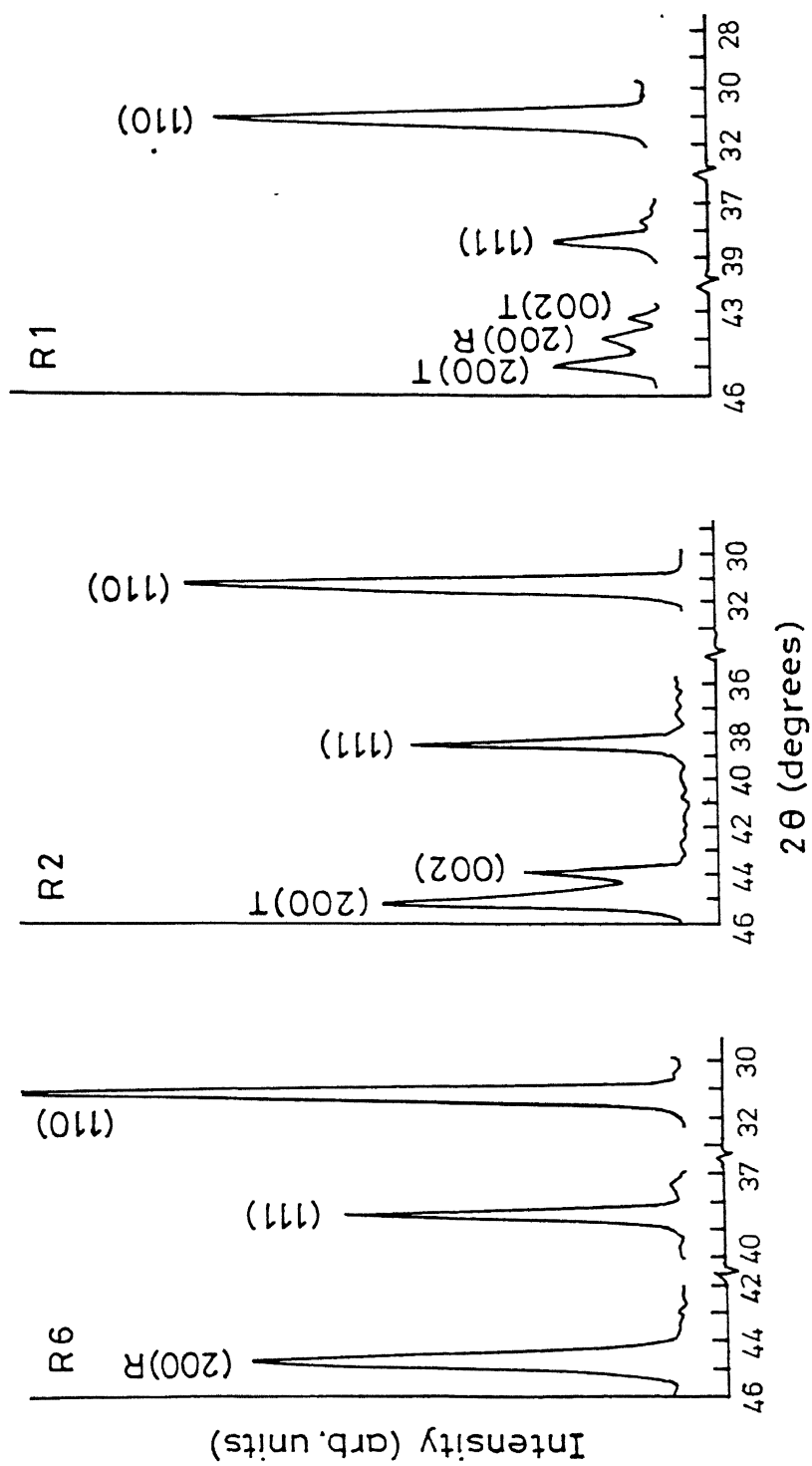
Slow scan XRD pattern of samples (a) R6
(rhombohedral) (b) R2 (tetragonal) and (c) R1
(rhombohedral + tetragonal)
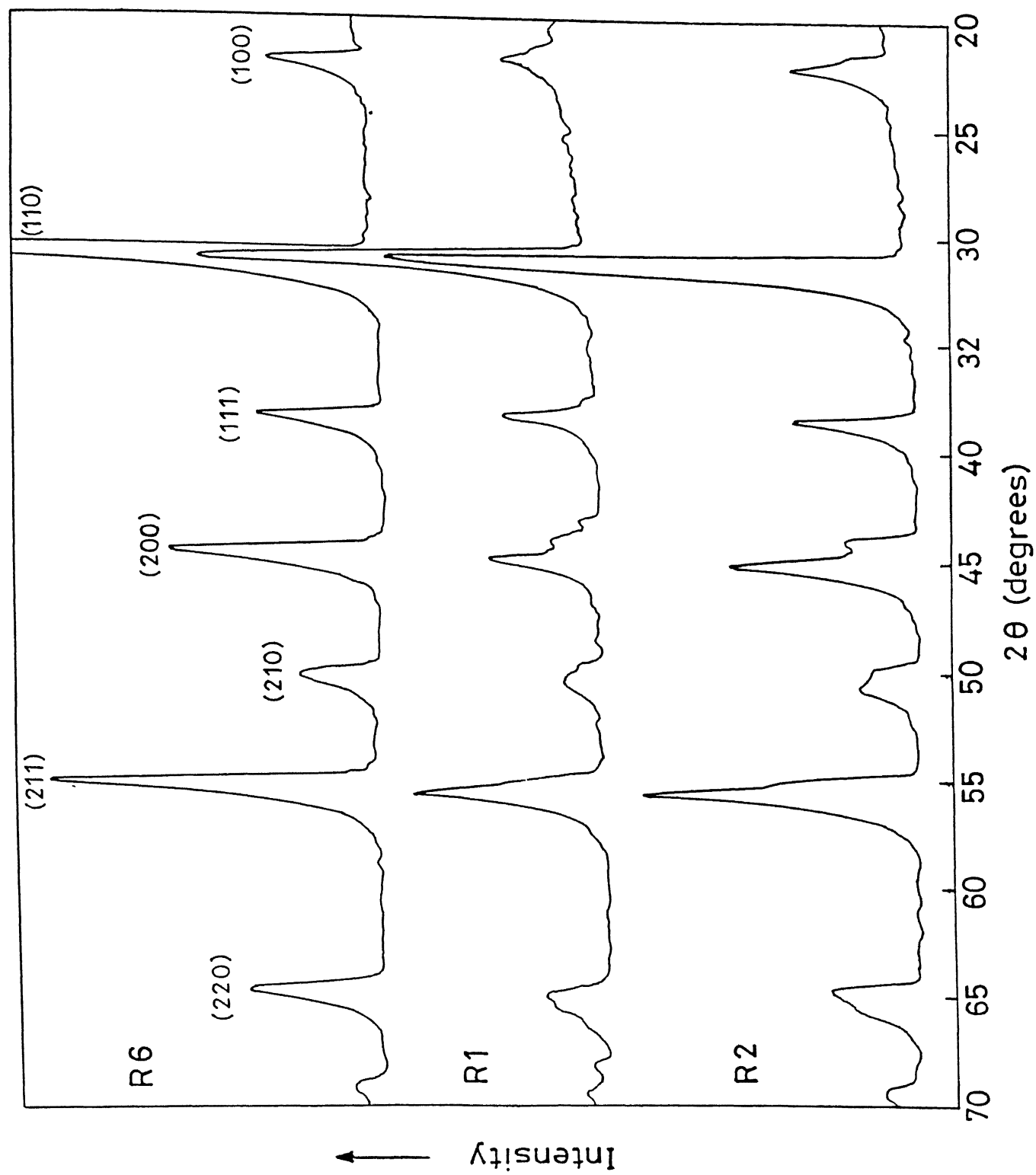
FIG. 4.3

FIG. 4.4   X-ray pattern of samples R6, R1 and R2.

composition (Fig. 4.3). The other sample had similar patterns and showed phases as listed in Table 4.6.

4.4   PIEZOELECTRIC PROPERTIES

It has been observed that when the tetragonality decreases the average d_{33} values (Table 4.7) get higher obviously because a greater amount of the sample mass has a chemical composition closer to that at the MPB. d_{33} values are higher for the composition which does not contain Al_2O_3.   Some samples broke during poling and could not be poled due to large strains generated during application of voltage.   Dielectric constant values (Table 4.7) before poling are higher than after poling. Maximum dielectric constant obtained was 902 for R6.

The variation of reactance with frequencies for the 16 sets of samples is obtained from impedance analyzer and some of them are shown in Fig.4.5, 4.6, 4.7 and 4.8.   All the poled samples responded well to the impedance analyzer.   The values of resonant, antiresonant frequencies and mechanical quality factor (Qm) are listed in Table.4.7.   Free relative dielectric constant (K_{33}^T), elastic compliance at constant electric field (S_{11}^E), electromechanical coupling coefficients (k_p, k_{31}, k_{33}), longitudinal voltage coefficient (g_{33}), frequency constant (F.C.) are calculated and result are given in Table 4.7.

The values of mechanical quality factor (Qm) obtained are in range of 63 to 235.   These values are low.   Electromechanical coupling coefficient values obtained are in the range of 0.27 to 0.45.

In our experiment we have added four dopants and also their
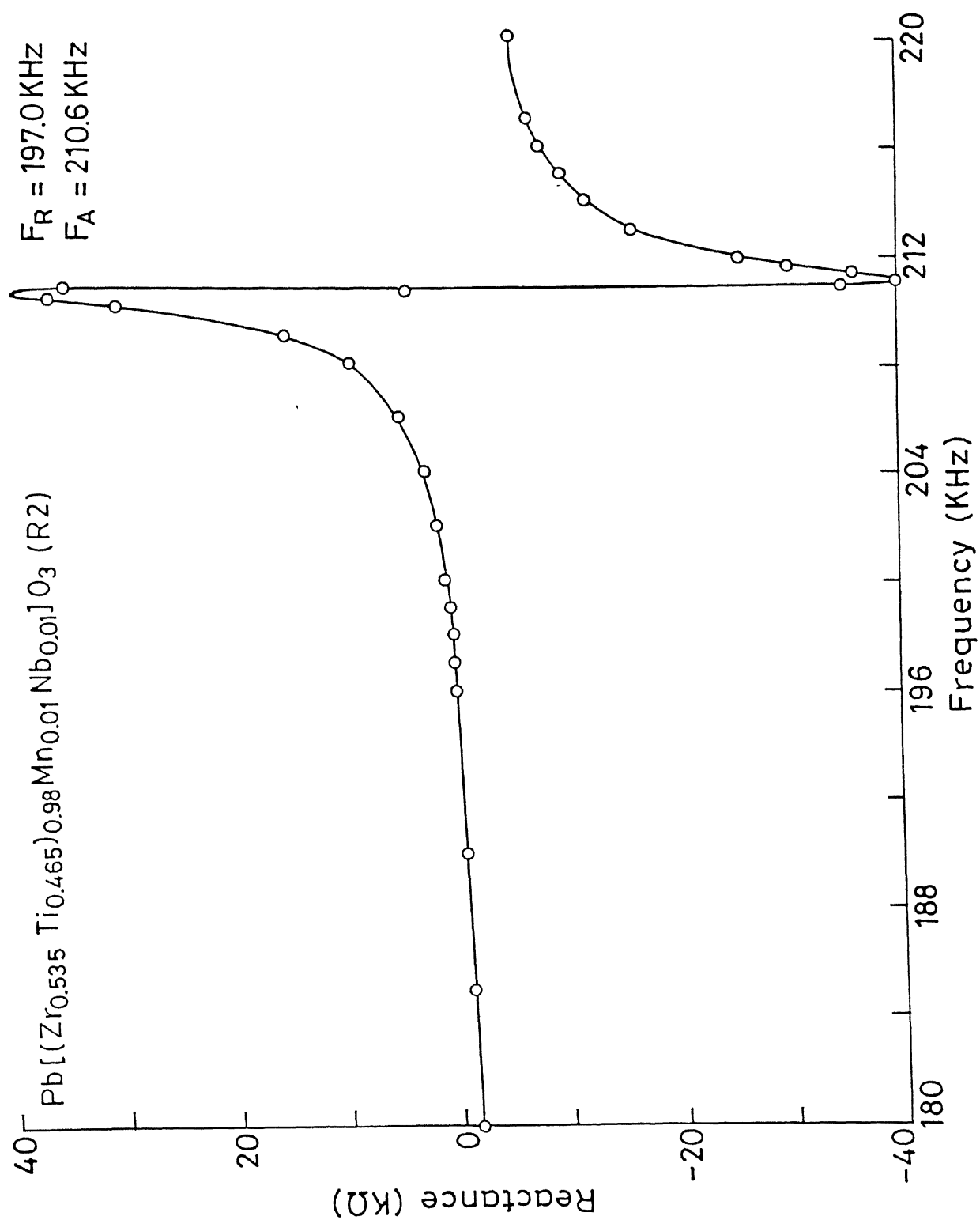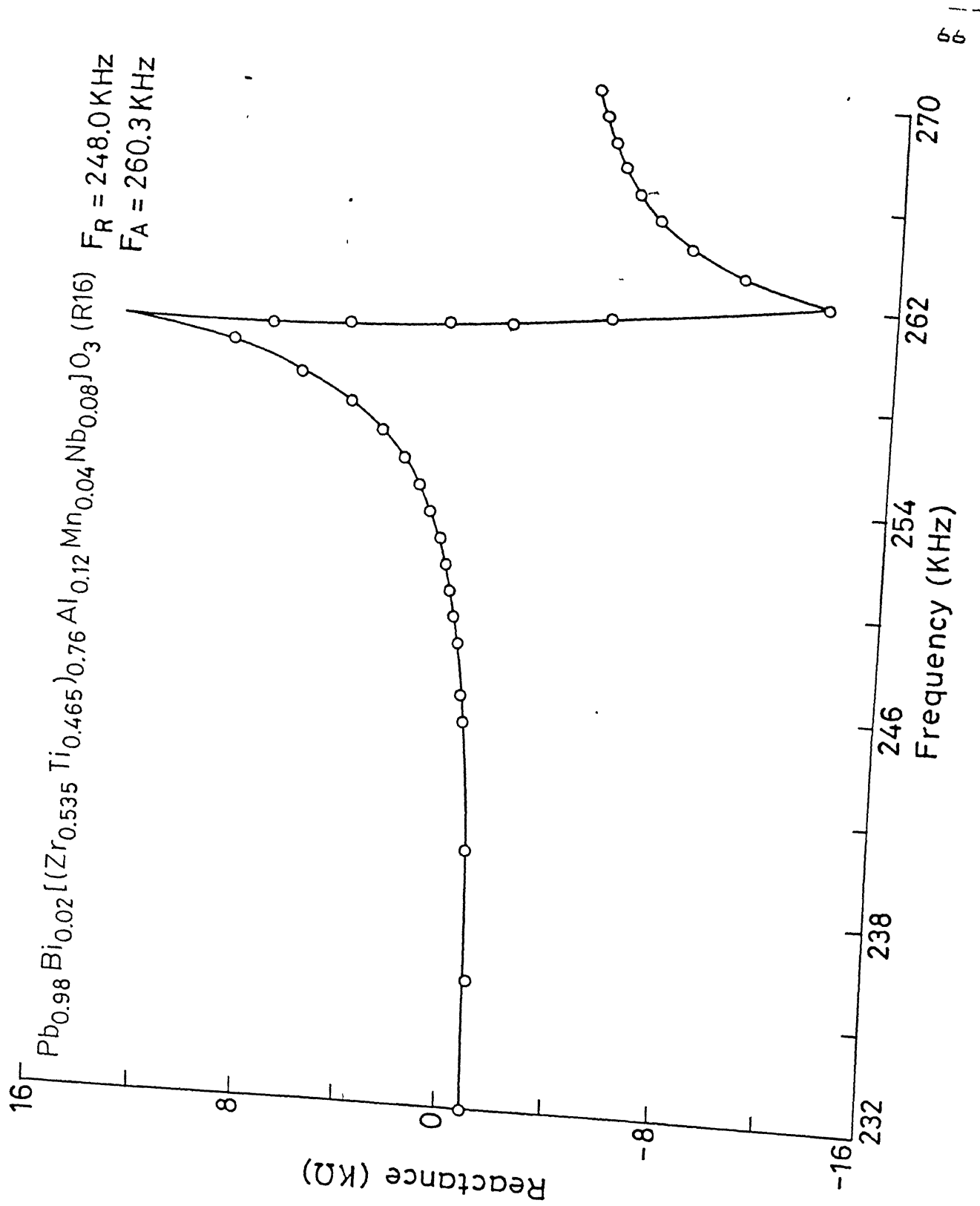
Pb[(Zr$_{0.535}$ Ti$_{0.465}$)$_{0.98}$Mn$_{0.01}$Nb$_{0.01}$]O$_3$ (R2)

F$_R$ = 197.0 KHz
F$_A$ = 210.6 KHz

FIG. 4.5   Variation of Reactances with frequencies

$Pb_{0.98}Bi_{0.02}[(Zr_{0.535}Ti_{0.465})_{0.76}Al_{0.12}Mn_{0.04}Nb_{0.08}]O_3$ (R16)

$F_R = 248.0\,KHz$

$F_A = 260.3\,KHz$

Frequency (KHz)

Reactance (KΩ)

Fig. 4.6   Variation of Reactances with frequencies

$Pb[(Zr_{0.535} Ti_{0.465})_{0.88} Mn_{0.04} Nb_{0.08}] O_3$ (R15)

$F_R = 242.0$ KHz

$F_A = 257.6$ KHz

Reactance (KΩ)

Frequency (KHz)

FIG. 4.7   Variation of Reactances with frequencies

$Pb_{0.98}Bi_{0.02}[(Zr_{0.535}Ti_{0.465})_{0.76}Al_{0.12}Mn_{0.04}Nb_{0.08}]O_3$ (R14)

$F_R = 250.4 \, KHz$

$F_A = 265.2 \, KHz$
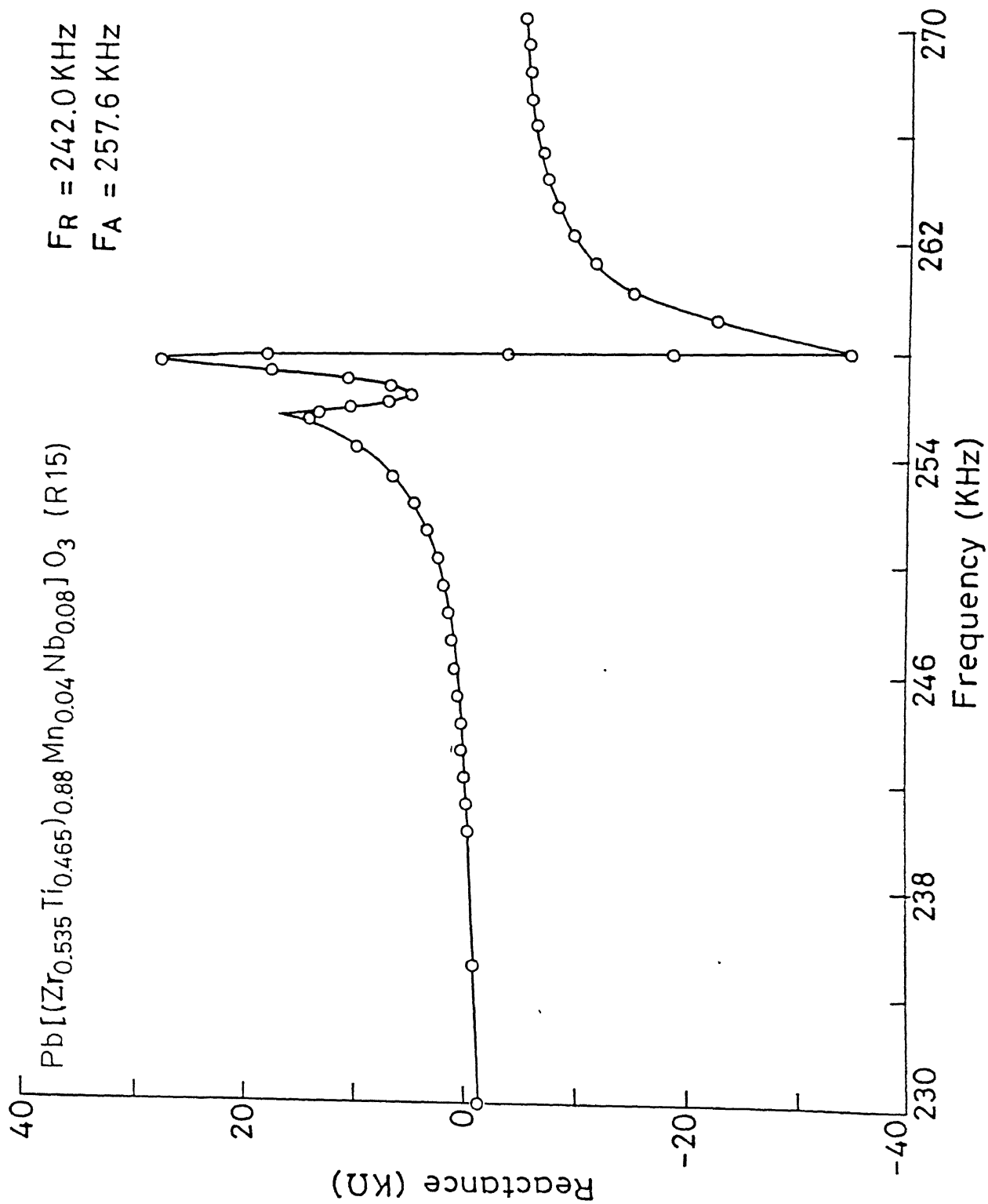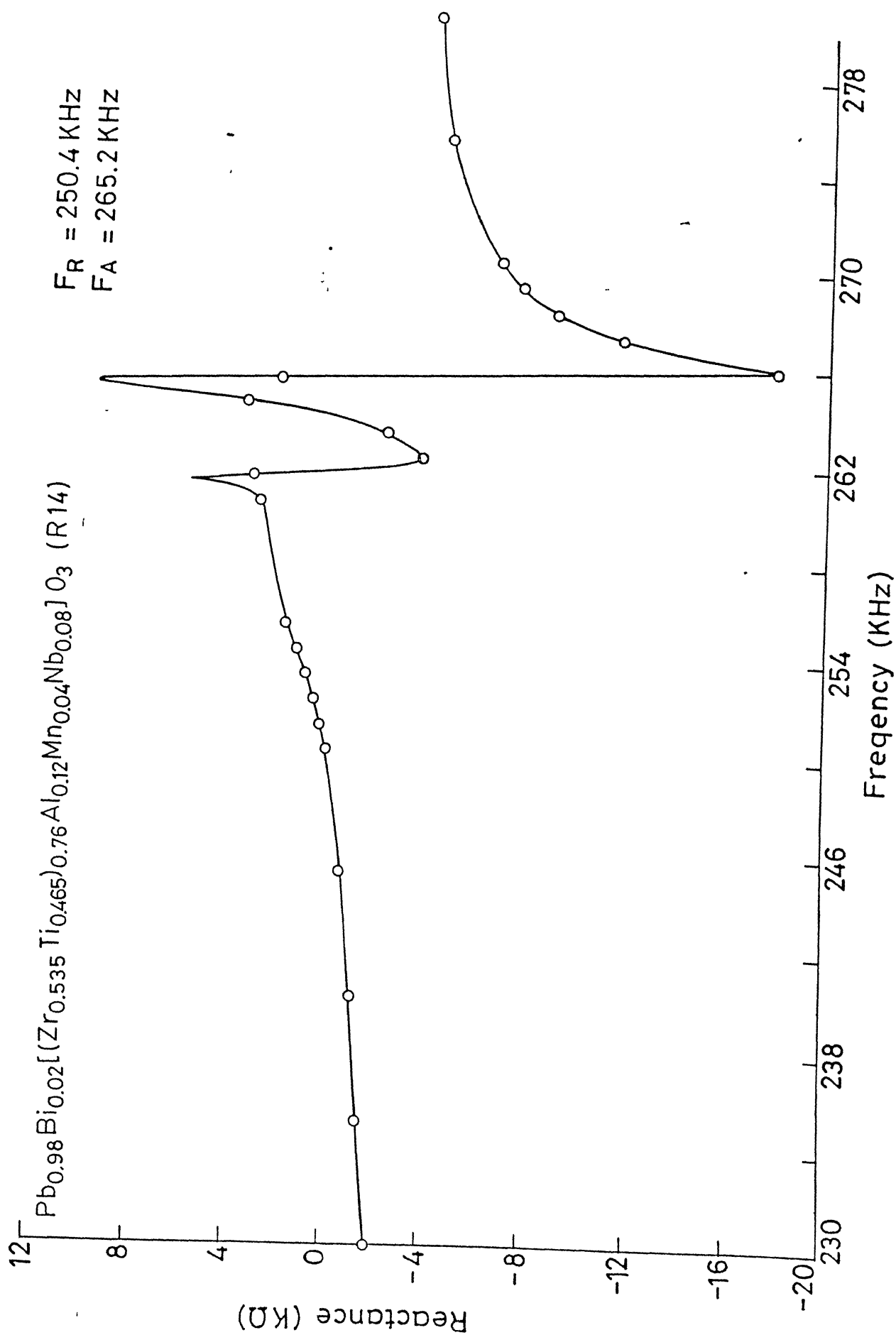
FIG.4.8   Variation of Reactances with frequencies

68

atom fractions are varied all at a time. There are 8 sets of different composition. There are no similarities between any two sets of composition. But among the dopants some are donors and some are accepters. Thus Nb_2O_5, Bi_2O_3 are donors and Al_2O_3 acts as an accepter.

Donor doped material creates Pb^{+2} vacancies. These vacancies facilitate domain wall motion with the application of very small electrical field or mechanical stresses. Thus it increases both elastic and dielectric compliance and loss factor. Also vacancies in Pb^{+2} position reduce the local stress in the domains. Thus domain can easily switch upon application or removal of the field. The cese of switching is related to relatively low coercive field and squareness of hysteresis loops. So mechanical quality factor Qm decreases with decrease of internal friction and hysteresis. Poling is easier for donor doped PZT material. As donor doped PZT materials show saturated normal hysteresis loops just after the application of field, they are ineffective in generating internal bias field and also ineffective in stabilising the polarization. In our experiment sets R2, R4, R8, R6, R12, R10, R15, R13 are mainly donor doped PZT material. Thus we find that they have high dielectric constant ranging from 510 to 902 at 1KHz. Values of Qm is also low except R2. This may be due to the presence of MnO_2 which increases the Qm value somewhat by creating space charge which pins the domain wall motion and stabilizes the domains. Also R8, R12, R10 could not be poled. Poling is difficult due to the restricted domain wall motions.

But in the case of accepter doped PZT materials vacancies in

the oxygen position will tend to shrink cell size. This shrinkage and distortion of cells is responsible for increasing mechanical quality factor Qm, increasing coercive force and lowering dielectric constant. Oxygen vacancies create large amount of space charges which slowly moves to the domain walls by diffusion, pin the walls and stabilize the domains. Thus domain wall motion is suppressed and internal friction due to this motion decreases. Thus accepter doped PZT materials show unsaturated constricted hysteresis loops due to the existence of internal bias field. Poling is carried on accompanied by the domain wall motion. So for accepter doped PZT internal bias field affects on the poling process.

In the run numbers R1, R7, R5, R3, R11, R9, R16, R14 both accepter and donors are present. They have low dielectric constant value. R5, R11, R9 could not be poled. But none of them has high mechanical quality factor (Qm) value. For filter ceramics mechanical losses should be as low as possible and consequently the Qm should be as high as possible. Mechanical and electrical losses in soft piezoceramics mainly arise due to vibration of domain walls and their interaction with lattice point defects. Mechanical losses in piezoelectric material is related to electrical conductivity (σ) which is discussed in chapter 1.9. σ of Mn doped ceramics is far higher than that of ceramics doped with donors or complex oxides. Mn sometimes shows anomalously large dielectric losses due to inhomogeneous high conductivities at grain boundaries. So the value of Qm for Mn doped ceramics is low. Also Mn gives stabilising effect, i.e. it gives high

stability with respect to frequency constant which makes them very useful in frequency filters.

Electromechanical coupling coefficient values for all the sets are quite good. All the composition prepared are near the MPB. MPB is of special interest because the permittivity and k_p reach their peak values. For all PZT ceramics the dielectric, piezoelectric and elastic properties and their temperature coefficients are closely related to the various ferroelectric phase transitions. Spontaneous polarization in Rhombohedral phase is more favourable than in tetragonal phase. Also spontaneous strain is less in Rhombohedral than in tetragonal phase.

4.5 OPTIMIZATION STUDIES

MODEL FITTING

The following first order model has been fitted to the experimental data.

$$\hat{Y} = \hat{b}_o + \hat{b}_1 x_1 + \hat{b}_2 x_2 + \hat{b}_3 x_3 + \hat{b}_4 x_4 + \hat{b}_5 x_5 + \hat{b}_6 x_6$$

where $\hat{b}_o \ldots \hat{b}_6$ are the best fitted values of coefficients, x_i is the ith variable in its coded form and $\hat{Y}$ is the predicted value of the response. The coefficients can be estimated by the least square technique as

$$\underline{\hat{b}} = (\underline{X}^T \underline{X})^{-1} \underline{X}^T \underline{Y}$$

Table 4.1   : The 2^{6-2} First Order (First Move) Design Matrix and values of the Responses

| RUN NO. | FACTORS IN CODED FORM | | | | | | VALUES OF | RESPONSES |
	X_1	X_2	X_3	X_4	X_5 (X_1X_3)	X_6 (X_1X_4)	DIELECTRIC CONSTANT (BEFORE POLING)	MECHANICAL QUALITY FACTOR
1	+	+	+	−	+	−	623	109.78
2	+	+	−	−	−	−	522	235.02
3	−	−	−	−	+	+	579	86.16
4	+	−	−	−	−	−	510	109.13
5	−	+	−	−	+	+	405	0
6	−	−	+	−	−	+	902	63.40
7	+	−	+	−	+	−	598	42.90
8	−	+	+	−	−	+	639	0
9	−	−	−	+	+	−	525	0
10	+	−	−	+	−	+	642	0
11	−	+	−	+	+	−	451	0
12	+	+	−	+	−	+	667	0
13	−	−	+	+	−	−	540	118.83
14	+	−	+	+	+	+	543	117.02
15	−	+	+	+	−	−	533	81.59
16	+	+	+	+	+	+	502	119.61
				Repeat Trials				
17	+	−	−	−	−	−	486	180.20
18	+	−	−	−	−	−	520	110.50
19	+	−	−	−	−	−	522	109.60

where $\underline{X}$ is the design matrix. $\underline{X}^T$ is the transpose of the design matrix. $\underline{Y}$ is the vector responses and $\hat{\underline{b}}$ is the vector of coefficients. The details of the method are given by Draper and Smith [36]. This is then tested for model adequacy by a Lack-of-fit F test. With the experimental results as given in Table.4.1, the fitted first order models for dielectric constant and mechanical quality factor are given below by equations (4.1) and (4.2).

$$\hat{Y}_{D.C.} = 56.6 - 0.56x_1 - 2.34x_2 + 4.385x_3 - 1.58x_4 - 3.79x_5 + 4.37x_6 \qquad 4.1$$

$$\hat{Y}_{Qm} = 7.92 + 3.85x_1 + 0.57x_2 + 0.75x_3 - 0.83x_4 - 0.83x_5 + 1.37x_6 \qquad 4.2$$

where $\hat{Y}_{DC}$, $\hat{Y}_{Qm}$ represent the predicted values of dielectric constant, mechanical quality factor, respectively. The lack of fit F tests for the above models are shown in Table 4.2 and 4.3 respectively. A model calculation of the analysis of variance (ANOVA) for conducting the Lack-of-fit F test has been done using NAG LIBRARY ROUTINE (as given in Appendix 2).

It is observed from Table 4.2 and 4.3 that a simple first-order model is not adequate for describing the dielectric constant and mechanical quality factor data. Hence a higher order model incorporating cross-product terms have been proposed and tested for Lack-of-fit F-test. This is given in Table 4.4 and .5.

Table 4.2:   First order Response Surface Strategy (First Move) :

Test for the Adequacy of the Model for Dielectric

Constant

$$\hat{Y}_{D.C.} = 56.6 - 0.56x_1 - 2.34x_2 + 4.385x_3 - 1.58x_4 - 3.79x_5 + 4.37x_6$$

ANOVA

Source	Degrees of freedom	Sum Square	Mean Square	F- Value
Model	7	24.5	3.51	4062
Fit	8	0.409	0.051	59.1
Error	4	0.0035	0.000864	
	Total 19			

$F_{0.01}(4,8) = 14.80$

Therefore, Model is not adequate.

Table 4.3.   : First order Response Surface Strategy (First Move)

Test for the Adequacy of the Model for Qm

$$\hat{Y}_{Qm} = 7.92 + 3.85x_1 + 0.57x_2 + 0.75x_3 - 0.83x_4 - 0.83x_5 + 1.37x_6$$

Source	DOF	Sum Square	Mean Square	F - Value
Model	7	0.609	0.087	1000
Fit	8	0.126	0.0158	182
Error	4	0.004	0.000868	
Total	19			

$F_{0.01}(4,8) = 14.80$

Model is not adequate.

The cross product terms which have influence on dielectric constant value are given below with the values of the coefficients,

b_0 = 572.5 b_2 = -29.64 b_3 = 37.62

b_4 = -22.01 b_6 = 37.49 b_7 = 35.12

$b_8 = -44.14 \qquad b_{10} = 17.51 \qquad b_{11} = -58.5$

Hence a better model can be proposed incorporating the above terms. The model then takes the following form,

$$\hat{Y}_{D.C.} = 572.5 - 29.64x_2 + 37.62x_3 - 22.01x_4 + 37.45\ x_6 +$$
$$+ 35.12\ x_1x_2 - 44.14x_1x_3 + 17.51x_4x_2 - 58.5x_1x_4x_5$$

Table 4.4 : First Order Response Surface Strategy (Second Move) : Test for the Adequacy of the Model for Dielectric Constant

Source	DOF	Sum Square	Mean Square	F - Value
Model	9	2490.00	276.00	3200
Fit	6	6.07	1.01	11.7
Error	4	0.346	0.086	
Total	19			

$F_{0.01}(4,6) = 15.21$

Therefore, model is adequate.

Similarly for Qm, proposed model even with cross-product terms does not satisfy the Lack-of-fit F-test. Anova Model with lowest F-value achieved is shown value,

$$\hat{Y}_{Qm} = 78.55 + 8.11x_3 - 7.65x_4 - 13.01x_6 + 30.27x_1x_4x_5 +$$
$$18.28x_4x_6 + 21.19x_2x_4x_6$$

Table 4.5 : First Order Response Surface Strategy (Second Move) : Test for the Adequacy of the Model for Qm

Source	DOF	Sum Square	Mean Square	F - Value
Model	7	69.1	9.367	1140
Fit	8	6.48	0.560	64.5
Error	4	0.0347	0.00868	
Total	19			

$F_{0.01}(4,8) = 14.80$

Therefore, model is not adequate.

OPTIMIZATION:

Of the above responses, dielectric constant of the sample was selected as the response to be optimized with respect to the independent variables. Thus data for the mechanical quality factor was also processed but no adequate model has been found using analysis of variance (ANOVA). As a result it is not possible to propose any optimised set of independent variables, so that the response mechanical quality factor can be maximised.

Coded value of the independent variables of sample no. R6 has been fitted into the adequate model of dielectric constant. The value of response i.e. dielectric constant comes out to be 854.49. This value is very much close to the experimental value obtained (902).

To check the model further a sample was prepared taking all the independent variables as x_1 = 4 hrs, x_2 = 1260°C, x_3 = 0.01, x_4=0.039, x_5=0.12, x_6 = 0.02. The value of dielectric constant obtained was 546. The result was also close to the value obtained from the model theoretically which was 559.94.

Unconstrained maximization was not done for getting maximum value of dielectric constant. This needs to be studied later.

Table 4.6 : % Theoretical Density, % Pb Loss and Phases

COMPOSITION DOPANTS CONCENTRATION (ATOM FRACTION)				SINT. TIME (hrs)	SINT TEMP. (RUN NO) (°C)	% Pb LOSS	% THEORET. DENSITY	PHASE ANALYSIS
Nb	Mn	Al	Bi					
0.08	0.01	0.12	0	4	1260 (R1)	7.80	96.83	R+T
					1220 (R7)	5.58	95.38	R
0.01	0.01	0	0	4	1260 (R2)	4.36	91.86	T
					1220 (R4)	-0.37	97.60	R
0.01	0.01	0.12	0.02	2	1260 (R5)	5.52	88.95	R
					1220 (R3)	4.69	91.50	R+T
0.08	0.01	0	0.02	2	1260 (R8)	2.71	98.11	T
					1220 (R6)	-0.28	97.30	R
0.01	0.04	0.12	0	2	1260 (R11)	7.95	91.49	R
					1220 (R9)	2.46	94.10	R
0.01	0.04	0	0.02	4	1260 (R12)	3.21	97.21	T
					1220 (R10)	-0.34	98.30	R
0.08	0.04	0	0	2	1260 (R15)	3.03	96.63	R
					1220 (R13)	-0.04	90.28	R
0.08	0.04	0.12	0.02	4	1260 (R16)	7.82	94.97	R+T
					1220 (R14)	4.19	95.26	R

SAMPLE DESCRIPTION	AVG. d_{33} $(10^{-12}C/N)$	DIELECTRIC CONST. (at 1 KHz)		fr (Khz)	fa (KHz)	Kp	Q_m
		BEFORE POLING	AFTER POLING				
08011200/1260/4	151	623	619	242.6	254.6	0.35	109.78
08011200/1220/4	138	598	436	224.6	235.4	0.35	42.90
01010000/1260/4	160	522	354	197.0	210.6	0.40	235.02
01010000/1220/4	179	510	279	224.6	244.0	0.45	109.13
01011202/1260/2	*	405	–	–	–	–	–
01011202/1220/2	123	579	464	199.1	204.4	0.27	86.16
08010002/1260/2	*	639	–	–	–	–	–
08010002/1220/2	161	902	790	216.5	228.5	0.36	63.40
01041200/1260/2	*	451	–	–	–	–	–
01041200/1220/2	*	525	–	–	–	–	–
01040002/1260/4	*	667	–	–	–	–	–
01040002/1220/4	*	642	–	–	–	–	–
08040000/1260/2	139	533	383	242.0	257.6	0.36	81.59
08040000/1220/2	141	540	374	248.0	260.4	0.35	118.83
08041202/1260/4	142	502	373	248.0	260.3	0.35	119.61
08041202/1220/4	123	543	388	250.4	265.2	0.36	117.02

* Samples could not be poled.

Table 4.7 : Piezoelectric Properties (continued)

RUN NO.	K^T_{33}	g_{33} (V-m/N)	k_{33}	k_{31}	d_{31} $(10^{-12}C/N)$	s^E_{11} $(10^{-12}m^2/N)$	F.C. (fr x r) KHz m
R1	705.41	0.024	0.34	0.20	53.15	10.77	1.191
R7	496.86	0.031	0.33	0.20	44.54	10.74	1.201
R2	421.43	0.043	0.38	0.23	51.45	12.90	1.116
R4	349.84	0.057	0.42	0.26	45.20	10.15	1.222
R3	500.48	0.027	0.25	0.16	37.87	12.95	1.118
R6	907.63	0.020	0.35	0.21	63.81	11.26	1.161
R15	440.03	0.035	0.37	0.21	42.74	10.42	1.212
R13	426.21	0.037	0.33	0.20	41.40	10.82	1.226
R16	425.07	0.037	0.33	0.20	40.46	10.36	1.226
R14	445.77	0.031	0.36	0.21	42.22	10.04	1.243

CHAPTER 5
CONCLUSION AND FURTHER SCOPE OF RESEARCH

In the present experiments four dopants were selected for doping of PZT so as to study their effect with a view to arrive at compositions which may be suitable for application in filters. A design of experiments approach was used. The main parameter which was aimed to be optimized was the mechanical quality factor Q_m. A set of 16 experiments were designed and conducted based on a fractional factorial design.

It was found that out of 16 sets, in R5, R8, R9, R10, R11, R12 sets, the grain size of the samples was very large so as to make it impossible to pole the samples. The Q_m data for these sets therefore could not be obtained. For the purpose of analyzing the data using the response surface methodology (RSM) the value of Q_m for the experiments was assumed to be zero. However, this did not help because the data could not be fitted to a model with reasonable degree of fit. Instead, the dielectric constant of unpoled samples was used as the variables to be analyzed using the RSM. This was successfully done. An arbitrary composition was then selected and a sample prepared and its dielectric constant measured. The measured value was found to be in reasonable agreement with the value predicted by the model. Thus it appears possible to design composition with desired dielectric constant using the model developed.

This was an initial study to explore the possibility of using the design of experiments and RSM for PZT ceramics. Further work may be in the following directions:

1. The data should be used to carry out and unconstrained maximization of the dielectric constant and the predicted value should be verified by experiment.

2. Another set of dopants should be selected, preferably only one or two at a time and optimization studies should be performed sequentially starting with the most important parameter followed by less important parameters for filter.

REFERENCES

1. Cady, W.G.; "Piezoelectricity", McGraw-Hill, New York (1946).

2. Mason, W.P.; "Piezoelectric Crystals and Their Application to Ultrasonics", Van Nostrand, New York (1950).

3. Buchanan, R.C.; "Ceramic Materials for Electronics Processing, Properties and Application", Marcel Dekker, Inc., New York and Basal, 1986.

4. Jaffe, B., Cook, W.R., Jr. and Jaffe, H.; "Piezoelectric Ceramics", Academic Press, New York, 1971.

5. Galasso, F.S.; Structure, Properties and Preparation of Perovskite type Compounds, Pergamon Press, London (1969).

6. Jaffe, B., Roth, R.S. and Marzullo, S.; "Piezoelectric Properties of Lead Zirconate - Lead Titanate Solid Solution Ceramics", J. Appl. Phys., 25, 909 (1954).

7. Sawaguchi, E.; "Ferroelectricity vs. Anti Ferroelectricity in the Solid Solution of $PbZrO_3-PbTiO_3$", J. Phys. Soc. Japan, 8, 615 (1953).

8. Arigur, P. and Benguigui, L.; "Direct Determinatin of the Coexistance Region in the Solid Solution $Pb(Zr_xTi_{1-x})O_3$" J. Phys. D., 8, 1856 (1975).

9. Matsuo, Y. and Sasaki, H.; "Formation of Lead Zirconate - Lead Titanate Solid solution", J. Am. Ceram. Soc., 48 (6), 289 (1965).

10. Takahashi, M.; "Space Charge Effect in Lead-Zirconate - Titanate Ceramics Caused by the Addition of Impurities", Jap. J. Appl. Phys., 9, 1236 (1970).

11. Takahashi, S.; "Effects of Impurity Doping in Lead-Zirconate-Titanate Ceramics", Ferroelectrics, 41, 143 (1982).

12. Takahashi, S. and Takahashi, M.; "Effects of Impurities on the Mechanical Quality Factor of Lead Zirconate Titanate Ceramics", Jpn. J. Appl. Phys., 11, 31 (1972).

13. Lambeek, P.V. and Jonker, G.H.; "Ferroelectric Domain Stabilisation in $BaTiO_3$ by Bulk Ordering of Defects", Ferroelectrics, 22, 729 (1978).

14. Jonker, G.H. and Lambeck, P.V.; "On the Origin of the Electrooptical Effect in Pyroelectric Crystals", 21, 641 (1978).

15. Atkin, R.B. and Fulrath, R.M.; "Point Defects and Sintering of Lead Zirconate Titanate", J. Am. Ceram. Soc., 54, 265 (1971).

16. Takahashi, S.; "Internal Bias Field Effects in lead Zirconate Titanate Ceramics Doped with Multiple Impurities", Jpn. J. Appl. Phys., 20, 95 (1981).

17. Herbert, J.M.; "Ferroelectric Transducers and Sensors", Gordon and Breach Science Publishers, New York.

18. Tanaka, T.; "Piezoelectric Devices in Japan", Ferroelectrics, 40, 167 (1982).

19. Onoe, M.; "Crystal, Ceramic and Mechanical Filters in Japan", Proc. IEEE, 67, 75 (1979).

20. Thomann, H. and Wersing, W.; "Principles of Piezoelectric Ceramics for Mechanical Filters", Ferroelectrics, 40, 189 (1982).

21. Jonker, G.H.; "Nature of Aging in Ferroelectric Ceramics", J. Am. Ceram. Soc., 55, 57 (1972).

22. Portnikov, V.S., Pavlov, V.S. and Tukov, S.K.; "Internal Friction in Ferroelectric due to Interaction of Domain Boundaries", J. Phys. Chem. Solids, 31, 1785 (1970).

23. Liao Jie-Hau, Cheng Syh-Yuh and Wang Chieu-Min; "Influence Factors for the Temperature Characteristics of Piezoelectric Properties", Ferroelectrics, 106, 357 (1990).

24. Arlt, G. and Dederichs, H.; "Complex Elastic, Dielectric and Piezoelectric Constants by Domain Wall Damping in Ferroelectric Ceramics", Ferroelectrics, 29, 47 (1980).

25. Kittrel, J.R., Erjavee, J.; "Response Surface Methods in Heterogeneous Kinetic Modelling", Ind. Eng. Chem. Proc. Des. Dev., 7(3), 321 (1966).

26. Box, G.E.P., Hunter, W.G., Hunter, J.S.; "Statistics for Experiments", John Wiley & Sons: New York, Chapters 10 and 12, 1978.

27. Davis, O.L.; "The Design and Analysis of Industrial Experiments", Longman Group Limited: New York, Chapter 11, 1978.

28. Khuri, A.I., Cornell, J.A.; "Response Surfaces Designs and Analysis", Marcel Dekker, Inc.: New York, Chapters 1, 2, 3 and 5, 1987.

29. Adler, Yu, P., Markova, E.V., Granovsky, Yu, V.; "The Design of Experiments to Find Optimal Conditions", Mir Publishers: Moscow, 1975.

30. Cochran, W.G., Cox, G.M.; "Experimental Designs", (2nd ed.), John Wiley & Sons: New York, 1957.

31. Hill, W.J., Hunter, W.G.; "A Review of Response Surface Methodology : A Literature Survey, Technometrics", 8 (4), 571 (1966).

32. Rao, M.S., Iyengar, S.S.; in Computer Modelling of Complex Biological System, (Eds. S. S. Iyengar) CRC press, Inc., Boca Raton, Fla., USA, 29 (1984).

33. Draper, N.R., Smith, H.; "Applied Regression Analysis 2nd ed.", John Wiley & Sons: New York, 1 (1981).

34. Long Wu, Chung Chang Lie, Tienshau Wu, Chung Chuang Wei; "Effect of Rare Earth Oxide on the Properties of Piezoelectric Ceramics", Ferroelectrics, 41, 157 (1982).

APPENDIX 1

Measurement scheme for piezoelectric ceramics

Constants	Specimen and orientation	Measurement scheme, or calculation method
s^E_{11}, k_{31}, d_{31}	Bar plated on faces perpendicular to Z.	Resonance measurements of the length extensional mode.
s^D_{11}	Bar plated on faces perpendicular to Z.	From above, using $s^D_{11} = (1 - k_{31}^2)s^E_{11}$.
ϵ^T_{33}	Bar plated on faces perpendicular to Z.	Measurement of low-frequency capacitance.
k_{15}	Bar poled along Z, but with plating on faces perpendicular to X.	Overtones of thickness shear mode of the same bar as above, but with signal field along X.
ϵ^T_{11}	Bar poled along Z, but with plating on faces perpendicular to X.	Measurement of low-frequency capacitance.
ϵ^S_{11}	Bar poled along Z, but with plating on faces perpendicular to X.	Measurement of high-frequency (clamped) capacitance.
s^E_{44}	Bar poled along Z, but with plating on faces perpendicular to X.	$k_{15}^2 = 1 - \epsilon^S_{11}/\epsilon^T_{11}$.
d_{15}, s^E_{12}	Bar poled along Z, but with plating on faces perpendicular to X. Square plate with faces perpendicular to Z.	$s^E_{44} = s^D_{44}/(1 - k_{15}^2)$. Fundamental resonance frequencies of the two contour-extensional modes of a square plate.
	Square plate with faces perpendicular to Z.	$s^D_{12} = s^E_{12} - k_{31}^2 s^E_{11}$.
s^E_{33}, d_{33}, k_{33}	Bar plated on faces perpendicular to Z, and with length along Z.	Resonance measurements of length extensional mode.
s^D_{33}, k_p, d_{h}	Bar plated on faces perpendicular to Z, and with length along Z. Disk with faces perpendicular to Z.	$s^D_{33} = s^E_{33}/(1 - k_{33}^2)$. Resonance measurements of planar extensional mode.
	Disk with faces perpendicular to Z.	Resonance measurements of thickness extensional mode.
	Disk with faces perpendicular to Z.	Measurement of response to hydrostatic pressure.
	Disk with faces perpendicular to Z. Disk with faces perpendicular to Z. Calculation. Calculation.	$d_{33} = d_h - 2d_{31}$. Overtones f_t of thickness extensional mode. Calculated from $c^D_{33}, s^D_{13}, s^D_{11}$ and s^E_{33}. $s^E_{13} = s^D_{13} + d_{31}d_{33}/\epsilon^T_{33}$.
	Calculation.	$\epsilon^S_{33} = \epsilon^T_{33}\left[1 - \dfrac{k_p^2 + k_{33}^2 + 2Ak_pk_{33}}{1 - A^2}\right]$,
		where
	or	$A = \dfrac{\sqrt{2}s^E_{13}}{\sqrt{s^E_{33}(s^E_{11} + s^E_{12})}}$
	Plate with faces perpendicular to Z.	Measurement of high-frequency (clamped) capacitance.

Note: s_{13}, s_{12} and d_{31} are generally negative. k_p is taken to be positive when d_{31} is negative.

APPENDIX - 2

The program to analyse the data is given at the end of this Appendix. To run this program following is to be done:

Inputing of data :

The input data is to be entered in file sangita1 for dielectric constant and file sangita2 for Mechanical quality factor Q_m. To input the data type the following command at the $ prompt.

$ vi sangita1⏎

The screen will show the data presently stored in the file. The first few rows look like the following:

DATA FILE

19	11	'U'	'M'						
+1	+1	+1	−1	+1	−1	+1	....	−1	623
+1	+1	−1	−1	−1	−1	+1	....	+1	522
−1	−1	−1	−1	+1	+1	+1	....	+1	579
.	.	.	.	.	.	.	....	.	.
.	.	.	.	.	.	.	....	.	.
.	.	.	.	.	.	.	....	.	.
+1	−1	−1	−1	−1	−1	−1	....	+1	522

2
3
4
5
7
8
0
1

Change the values in this file as desired. At the end of the ile the numbers 2, 3, etc in a single column refer to B(2), B(3) tc. which are to be selected to get acceptable F value. Then at he end type the following :

:wq ↵

      Depending on whether the input file is sangita1 or sangita2 the name has to be accordingly changed in the program. To access the program listing type the following:

$ vi g02defe.f ↵

Now move the cursor to the paragraph under "GET THE INPUT DATA" near the beginning of the program and change the file name as required. To come out of the listing, press

ESc

and then type,

: wq ↵

Now to compile the program, type the following,

$ f77 +800 g02defe.f -lnag - 0 g02 ↵

Now to run the program type the following, $ g02 ↵

To see the output type the following,

$ vi out1 ↵ (when input file is sangita1) or

$ vi out2 ↵ (when input file is sangita2).

      The program does the first iteration using the constant B(0) and the first coefficient B(2) provided in this example. In the next iteration B(3) is also used and so on until the last iteration uses all the coefficients. The choice of coefficient can then be changed if the F value obtained is not acceptable.

NOTE :   In the program the input value of dielectric constant and Q_m are divided by 50 for convenience. The coefficient are therefore to be multiplied by 50.

```
***********************************************************************
* PROGRAM TO OBTAIN THE LINEAR LEAST SQUARE MODEL FITTING THE
* GIVEN EXPERIMENTAL DATA
* USES NAG SUBROUTINE    G02DEF
* PLEASE REFER TO DETAILED DOCUMENTATION IN NAG-14 REFERENCE MANUAL
* >>>>>>>>>>>>>>>>>>>>>>>><<<<<<<<<<<<<<<<<<<<<<<<<<<<<<
* THE FOLLOWING IS A LIST OF THE  DIFFERENT VARIABLES USED
* >>>>>>>>>>>>>>>>>>>>>>>><<<<<<<<<<<<<<<<<<<<<<<<<<<<<
*   NMAX                           >> MAX NO. OF EXPTL. PTS.
*   MMAX                           >> MAX NO. OF COEFFS.
*   B(MMAX)                        >> ARRAY OF COEFFICIENTS
*   COV                            >> UPPER TRIANGLE OF THE COVARIANCE
*                                     MATRIX
*   X(NMAX,MMAX)                   >> ARRAY OF INDEPENDENT VARIABLES
***********************************************************************
      implicit real *8 (a-h,o-z)
*       .. Parameters ..
      INTEGER          MMAX, NMAX
      PARAMETER        (MMAX=13,NMAX=20)
      INTEGER          NIN, NOUT
      PARAMETER        (NIN=25,NOUT=16)
*       .. Local Scalars ..
      DOUBLE PRECISION RSS, RSST, TOL
      INTEGER          I, IDF, IFAIL, INDX, IP, IRANK, J, M, N
      integer          IDX(MMAX+1)
      LOGICAL          SVD
      CHARACTER        MEAN, WEIGHT
      CHARACTER *12    INFIL
*       .  Local Arrays .
      DOUBLE PRECISION B(MMAX), COV(MMAX*(MMAX+1)/2), P(MMAX*(MMAX+2)),
     +                 Q(NMAX,MMAX+1), SE(MMAX), WK(MMAX*MMAX+5*MMAX),
     +                 WT(NMAX), X(NMAX,MMAX), XX(3)
*       .  External Subroutines ..
      EXTERNAL         F06FBF, G02DDF, G02DEF,FUN
*       .  Executable Statements ..
***********************************************************************
*     GET THE INPUT DATA
***********************************************************************
*     WRITE (NOUT,*) 'MODEL FITTING RESULTS '
*     TYPE*,'GIVE THE DATAFILE NAME'
*     READ(*,*)INFIL
*     WRITE(*,*)'THE INPUT FILE IS ',INFIL
      open(unit = nin, file = 'sangita2')
      open(unit = nout, file = 'out2')
***********************************************************************
*     Skip heading in data file
***********************************************************************
      READ (NIN,*)
      READ (NIN,*) N, M, WEIGHT, MEAN
***********************************************************************
*     IF WEIGHT IS 'U', THEN UNWEIGHTED LEAST SQUARES DONE
***********************************************************************
      IF (N.LE NMAX .AND  M LT.MMAX) THEN
         IF (WEIGHT.EQ.'W'   OR. WEIGHT.EQ 'w') THEN
            DO 20 I = 1, N
               READ (NIN,*) (X(I,J),J=1,M), Q(I,1), WT(I)
***********************************************************************
*     IN CASE OF MRR DATA, Q HAS TO BE DIVIDED BY 20
***********************************************************************
*               Q(I,1) = Q(I,1)/20.0d0
   20       CONTINUE
         ELSE
            DO 40 I = 1, N
               READ (NIN,*) (X(I,J),J=1,M), Q(I,1)
***********************************************************************
*     IN CASE OF MRR DATA, Q HAS TO BE DIVIDED BY 20
```

```
*******************************************************************
              Q(I,1) = Q(I,1)/50 0d0
40            CONTINUE
         END IF
*******************************************************************
*   CALCULATION OF THE VARIOUS SUM SQUARES
*   FIRST >> SUMSQUARES OF EXPTL  DATA
*******************************************************************
         SSQM=0.0d0
         do I=1,N
         SSQM=SSQM+Q(I,1)**2
         ENDDO
*******************************************************************
*        WE OBTAIN THE MEAN FOR THE REPEATED RUNS   IN THE PROCESS
*        WE LOSE ONE DEGREE OF FREEDOM.
*******************************************************************
         SSQREP=0.0d0
*******************************************************************
*        IBEG IS THE STARTING RUN NO  FOR THE REPEATED RUNS
*******************************************************************
         IBEG = 15
         IEND = N
         do i=IBEG,IEND
         SSQREP = SSQREP + Q(I,1)
         ENDDO
*******************************************************************
*   THIS IS THE MEAN
*******************************************************************
         SMEAN=SSQREP/float(IEND-IBEG+1)
*******************************************************************
*        NEXT WE EVALUATE THE SUMSQ. OF REPEATED RUNS
*******************************************************************
         SSQREP=0.0d0
         do i=IBEG,IEND
         SSQREP = SSQREP + (Q(I,1)-SMEAN)**2
         ENDDO
*******************************************************************
*   THIS IS THE EXPERIMENTAL ERROR DEGREE OF FREEDOM
*******************************************************************
         DOFERR=float(IEND-IBEG)
*******************************************************************
*   THIS IS THE TOTAL DEGREE OF FREEDOM
*******************************************************************
         DOFTOT=FLOAT(N)
*******************************************************************
*   WE CALCULATE THE MEAN SQUARES FOR THE TOTAL AND THE EXP. ERR.
*******************************************************************
         AMSQT=SSQTOT/DOFTOT
         AMSQE=SSQREP/DOFERR
*******************************************************************
*        Set tolerance
*******************************************************************
         TOL = 0 000001D0
         IP = 0
         IF (MEAN EQ 'M' .OR. MEAN EQ.'m') THEN
*
             CALL F06FBF(N,1.0D0,X(1,MMAX),1)
*
             IFAIL = 0
*
             CALL G02DEF(WEIGHT,N,IP,Q,NMAX,P,WT,X(1,MMAX),RSS,TOL,IFAIL)
*
             IP = 1
         END IF
         IDX(1) = 0
         II = 2
```

```
************************************************************************
*    WE READ THE COEFF  TO BE ADDED
************************************************************************
   60     READ (NIN,*) INDX
          IF (INDX GT 0) THEN
             IFAIL = -1
             IDX(II) = INDX
*
             CALL G02DEF(WEIGHT,N,IP,Q,NMAX,P,WT,X(1,INDX),RSS,TOL,IFAIL)
*
             IF (IFAIL EQ 0) THEN
                WRITE(nout,99993)'CASE ',IP
                IP = IP + 1
                WRITE (NOUT,*)
                WRITE (NOUT,99999) 'Variable', INDX, ' added'
                RSST = 0 0D0
                IFAIL = 0
*
             CALL G02DDF(N,IP,Q,NMAX,RSST,IDF,B,SE,COV,SVD,IRANK,P,
     +                     TOL,WK,IFAIL)
*
             IF (SVD) THEN
                WRITE (NOUT,*) 'Model not of full rank'
                WRITE (NOUT,*)
             END IF
************************************************************************
*   WE OBTAIN THE RESIDUAL SUM OF SQUARES
************************************************************************
                WRITE (NOUT,99998) 'Residual sum of squares = ', RSST
                WRITE (NOUT,99999) 'Degrees of freedom = ', IDF
                WRITE (NOUT,*)
                WRITE (NOUT,*)
     + 'Parameter      estimate       Std. error      t-value'
************************************************************************
*    THE DEGREES OF FREEDOM FOR THE MODEL = NO. OF COEFFICIENTS
************************************************************************
                DOFMOD=FLOAT(IP)
                WRITE (NOUT,*)
                DO 80 J = 1, IP
************************************************************************
*     HERE WE OBTAIN THE T- VALUES
************************************************************************
                   TTEST = B(J)/SE(J)
                   WRITE (NOUT,99997) IDX(J), B(J), SE(J),TTEST
   80           CONTINUE
************************************************************************
*    WE CALCULATE THE REMAINING SUM SQUARES
*    i e. SUMSQ  OF MODEL
************************************************************************
                SSQMOD=SSQM-RSST
************************************************************************
*    & SUMSQ. OF FIT (BY SUBTRACTION)
************************************************************************
                SSQLFT=RSST-SSQREP
                DOFRES=DOFTOT-DOFMOD
                DOFLFT=DOFRES-DOFERR
************************************************************************
*      NOW WE TACKLE THE MEAN SQUARES.
************************************************************************
                AMSQM=SSQMOD/DOFMOD
                AMSQR=RSST/DOFRES
                AMSQL=SSQLFT/DOFLFT
                AMSQT=SSQM/DOFTOT
                FMOD = AMSQM/AMSQE
************************************************************************
*     WE OBTAIN THE F- VALUE
```

```
*********************************************************************
                 FVAL= AMSQL/AMSQE
*********************************************************************
*      AND CONSTRUCT THE ANOVA TABLE
*********************************************************************
              WRITE(nout,*)'    '
              write(nout,99994)'     *************************'
              WRITE(nout,99994)'     ANOVA FOR THE PRESENT MODEL'
              write(nout,99994)'     *************************'
              write(nout,99994)
     *  'Source   DOF     Sum Square   Mean Square     F-Value'
       write(nout,99995) 'MODEL', DOFMOD, SSQMOD, AMSQM , FMOD
       write(nout,99995) 'FIT ', DOFLFT, SSQLFT, AMSQL , FVAL
       write(nout,99996) 'ERROR', DOFERR, SSQREP, AMSQE
       write(nout,99994)'_____
     +___'
       write(nout,99996) 'TOTAL', DOFTOT, SSQM,  AMSQT
       write(nout,99994)'_____
     +___'
       WRITE(nout,99994)'   '
              ELSE IF (IFAIL.EQ.3) THEN
                 WRITE (NOUT,*) ' * New variable not added *'
              ELSE
                 GO TO 100
              END IF
              II = II + 1
*********************************************************************
* PRESENT CASE OVER; NOW ADD THE NEXT COEFFICIENT AND START AFRESH
*********************************************************************
              GO TO 60
           END IF
        END IF
  100 CONTINUE
*********************************************************************
* IF YOU WANT THE PREDICTED VALUES OF THE DEPENDENT VARIABLE
* THEN THIS IS NEEDED
*                      ****BE CAREFUL****
* MODIFY THE SUBROUTINE FUN ACCORDINGLY BEFORE PROCEEDING WITH
*  THE NEXT PART OF THE PROGRAM
*********************************************************************
              NUMPT = 30
              type*,'DO YOU WANT TO OBTAIN THE FUNCTION VALUES?'
              type*,' 1>> YES; 2>> NO'
              read(*,*)IRESP
              IF(IRESP EQ.1)THen
*********************************************************************
* THE RESULTS ARE STORED IN A FILE CALLED var1
*********************************************************************
              open(unit=26,file='var1')
  101         type*,'WHICH VARIABLE YOU WANT TO VARY ? 1, 2, 3, 4, 5, 6?'
              read(*,*)IVAR
              if(ivar eq 1) THEN
              type*,'WHAT ARE THE VALUES AT WHICH YOU FIX X(2), X(3), X(4),
     +        X(5), X(6)'
              READ(*,*) XX(2), XX(3),XX(4),XX(5),XX(6)
              t1 = xx(2)
              t2 = xx(3)
              t3 = xx(4)
              t4 = xx(5)
              t5 = xx(6)
              ELSE IF (IVAR .EQ 2) THEN
              type*,'WHAT ARE THE VALUES AT WHICH YOU FIX X(1), X(3), X(4),
     +        X(5), X(6)'
              READ(*,*) XX(1), XX(3),XX(4),XX(5),XX(6)
              t1 = xx(1)
              t2 = xx(3)
```

```
                  t3 = xx(4)
                  t4 = xx(5)
                  t5 = xx(6)
                  ELSE IF (IVAR  EQ   3) THEN
                  type*,'WHAT ARE THE VALUES AT WHICH YOU FIX X(1), X(2), X(4),
     +            X(5), X(6)'
                  READ(*,*) XX(1), XX(2),XX(4),XX(5),XX(6)
                  t1 = xx(1)
                  t2 = xx(2)
                  t3 = xx(4)
                  t4 = xx(5)
                  t5 = xx(6)
                  ELSE IF (IVAR .EQ. 4) THEN
                  type*,'WHAT ARE THE VALUES AT WHICH YOU FIX X(1), X(2), X(3),
     +            X(5), X(6)'
                  READ(*,*) XX(1), XX(2),XX(3),XX(5),XX(6)
                  t1 = xx(1)
                  t2 = xx(2)
                  t3 = xx(3)
                  t4 = xx(5)
                  t5 = xx(6)
                  ELSE IF (IVAR .EQ. 5) THEN
                  type*,'WHAT ARE THE VALUES AT WHICH YOU FIX X(1), X(2), X(3),
     +            X(4), X(6)'
                  READ(*,*) XX(1), XX(2),XX(3),XX(4),XX(6)
                  t1 = xx(1)
                  t2 = xx(2)
                  t3 = xx(3)
                  t4 = xx(4)
                  t5 = xx(6)
                  ELSE IF (IVAR  EQ   6) THEN
                  type*,'WHAT ARE THE VALUES AT WHICH YOU FIX X(1), X(2), X(3),
     +            X(4), X(5)'
                  READ(*,*) XX(1), XX(2),XX(3),XX(4),XX(5)
                  t1 = xx(1)
                  t2 = xx(2)
                  t3 = xx(3)                                        \
                  t4 = xx(4)
                  t5 = xx(5)
                  ENDIF
*
                  type*,'VARYING x',IVAR,'  FROM 2.0d0 To 4 0d0'
                  write(26,*)NUMPT+1
                  write(26,99991)t1,t2
                  do kk1 = 1, NUMPT+1
                  xx(ivar) = 2 0d0+6 0D0*DBLE(KK1-1)/DBLE(NUMPT)
                  call fun(y,Xx,MMAX,B,6)
                  write(26.99992)Xx(ivar),y
                  ENDDO
                  type*,'WANT TO REPEAT THE FUNCTION CALCULATION?'
                  type*,' 1>> YES, 2>> NO'
                  reaD(*,*)IRESP
                  IF(IRESP   EQ   1) THEN
                  GO TO 101
                ENDIF
              ENDIF
          STOP
*
99999 FORMAT (1X,A,I4,A)
99998 FORMAT (1X,A,D13 4)
99997 FORMAT (1X,'B(',I3,')',3D15 4)
99996 FORMAT (1X,A,4X,F3 0,2(2X,D12 3))
99995 FORMAT (1X,A,4X,F3 0,3(2X,D12.3))
99994 FORMAT (1X,A)
99993 FORMAT (1X,A,I2)
99992 FORMAT (1x,F6 3. 5x. D15 6)
```

```
99991 FORMAT (1x,f4 1,1X,f4 1)
99990 FORMAT (1X,A,D15.4)
      END
*****************************************************************
      subroutine FUN(yfun,x,MMAX,B2,NVAR)
      implicit real *8 (a-h,o-z)
      DIMENSION B2(MMAX),x(NVAR)
C28 +
      YFUN =    B2(1) + B2(2)*X(3) + B2(3)*x(4)
     +          + B2(4)*x(5) + B2(5)*X(6)
     +          + B2(6)*X(1)*X(2) + B2(7)*X(1)*X(4)*X(5)
     *          + B2(8)*X(4)*X(6)
*     YFUN =    B2(1) + B2(2)*X(1) + B2(3)*x(3)
*     *          + B2(4)*x(1)**2 + B2(5)*X(2)**2
*     *          + B2(6)*X(1)**3 + B2(7)*X(3)**3 + B2(8)*x(1)**4
      RETURN
      END
*****************************************************************
```

CASE 1

Variable 2 added
Residual sum of squares =   7810E+02
Degrees of freedom =   17

Parameter   estimate   Std error   t-value

B(0)   1122E+02   .4980E+00   .2252E+02
B(2)   - 3607E+00   .4980E+00   -.7243E+00

        ****
        ANOVA FOR THE PRESENT MODEL
        ****
Source   DOF   Sum Square   Mean Square   F-Value
MODEL   2   .242E+04   .121E+04   .140E+05
FIT   13   .778E+02   .598E+01   .692E+02
ERROR   4.   346E+00   .864E-01

TOTAL   19   .249E+04   .131E+03
_____

CASE 2

Variable 3 added
Residual sum of squares =   6446E+02
Degrees of freedom =   16

Parameter   estimate   Std error   t-value

B(0)   1133E+02   4707E+00   2408E+02
B(2)   -.4788E+00   4707E+00   -.1017E+01
B(3)   .8662E+00   .4707E+00   .1840E+01

        ****
        ANOVA FOR THE PRESENT MODEL
        ****
Source   DOF   Sum Square   Mean Square   F-Value
MODEL   3   .243E+04   .810E+03   .938E+04
FIT   12   .641E+02   .534E+01   .618E+02
ERROR   4   .346E+00   .864E-01

TOTAL   19   249E+04   .131E+03
_____

CASE 3

Variable 4 added
Residual sum of squares =   .6294E+02
Degrees of freedom =   15

Parameter   estimate   Std error   t-value

B(0)   1130E+02   .4839E+00   .2335E+02
B(2)   -.4438E+00   .4839E+00   -.9172E+00
B(3)   .9012E+00   .4839E+00   .1862E+01
B(4)   -.2913E+00   .4839E+00   -.6021E+00

        ****
        ANOVA FOR THE PRESENT MODEL
        ****
Source   DOF   Sum Square   Mean Square   F-Value
MODEL   4   .243E+04   .608E+03   .704E+04
FIT   11   .626E+02   .569E+01   .659E+02
ERROR   4.   346E+00   .864E-01
_____

```
TOTAL      19        .249E+04        .131E+03
```

CASE 4

Variable   6 added
Residual sum of squares =   .5127E+02
Degrees of freedom =   14

```
Parameter      estimate        Std. error      t-value

B(  0)         .1139E+02       .4547E+00       .2504E+02
B(  2)        - 5308E+00       4547E+00       -.1167E+01
B(  3)         .8142E+00       4547E+00        .1791E+01
B(  4)        - 3783E+00       4547E+00       -.8320E+00
B(  6)         8117E+00        4547E+00        1785E+01
```

```
          *+++++++++++++++++*++*++*++*+*+*
          ANOVA FOR THE PRESENT MODEL
          *++++++++++++*+*+*+*+*+*+*+*+*+*
Source   DOF      Sum Square    Mean Square    F-Value
MODEL    5         244E+04        489E+03        566E+04
FIT      10       .509E+02        509E+01        589E+02
ERROR    4         346E+00       .864E-01

TOTAL    19       249E+04        131E+03
```

CASE 5

Variable   7 added
Residual sum of squares =   4275E+02
Degrees of freedom =   13

```
Parameter      estimate        Std. error      t-value

B(  0)         .1145E+02       .4329E+00       .2646E+02
B(  2)        - 5992E+00       .4329E+00      -.1382E+01
B(  3)         .7468E+00       .4329E+00       .1725E+01
B(  4)        -.4457E+00       .4329E+00      - 1030E+01
B(  6)         .7443E+00       .4329E+00       .1719E+01
B(  7)         6968E+00        .4329E+00       .1610E+01
```

```
          *******+*+**+*+*+*+***+**+*+*+*
          ANOVA FOR THE PRESENT MODEL
          *+*+*+*+*+*+*+*+*+*+***+*+***+*
Source   DOF      Sum Square    Mean Square    F-Value
MODEL    6         245E+04        409E+03       .473E+04
FIT      9         424E+02       .471E+01       .545E+02
ERROR    4         346E+00       .864E-01

TOTAL    19       249E+04        .131E+03
```

CASE 6

Variable   8 added
Residual sum of squares =   .3115E+02
Degrees of freedom =   12

```
Parameter      estimate        Std  error      t-value

B(  0)         1138E+02        .3861E+00       .2948E+02
B(  2)        - 5262E+00       .3861E+00      -.1363E+01
B(  3)         .3188E+00       .3861E+00       .2121E+01
B(  4)        - 3737E+00       .3861E+00      -.9679E+00
```

```
B(  6)           8163E+00 ᵃ        .3861E+00          .2114E+01
B(  7)           7688E+00          .3861E+00          .1991E+01
B(  8)        -  8162E+00          .3861E+00         -.2114E+01


          ****************************
          ANOVA FOR THE PRESENT MODEL
          ****************************
Source    DOF        Sum Square     Mean Square       F-Value
MODEL     7           246E+04        .352E+03          .407E+04
FIT       8.         .308E+02        .385E+01          .446E+02
ERROR     4.          346E+00        .864E-01
_____
TOTAL     19          249E+04        .131E+03
_____


CASE   7

Variable  10 added
Residual sum of squares =         2996E+02
Degrees of freedom =    11

Parameter      estimate        Std. error       t-value

B(   0)          1136E+02        .3968E+00        .2863E+02
B(   2)        -  5049E+00        3968E+00       -.1273E+01
B(   3)         .8401E+00        .3968E+00        .2117E+01
B(   4)        -.3524E+00        .3968E+00       -.8882E+00
B(   6)          8376E+00        3968E+00         .2111E+01
B(   7)          7901E+00        .3968E+00        1991E+01
B(   8)        -.7949E+00        .3968E+00       -.2003E+01
B(  10)          2624E+00        .3968E+00        .6614E+00


          ****************************
          ANOVA FOR THE PRESENT MODEL
          ****************************
Source    DOF        Sum Square     Mean Square       F-Value
MODEL     8.         .246E+04        308E+03           .357E+04
FIT       7          .296E+02        423E+01           .490E+02
ERROR     4.          346E+00   .    .864E-01
_____
TOTAL     19          249E+04        .131E+03
_____


CASE   8

Variable  11 added
Residual sum of squares =         6419E+01
Degrees of freedom =    10

Parameter      estimate        Std   error       t-value

B(   0)          1145E+02        .1932E+00        .5926E+02
B(   2)        -.5927E+00        .1932E+00       -.3068E+01
B(   3)          7523E+00        .1932E+00        3894E+01
B(   4)        -  4402E+00        1932E+00       -  2279E+01
B(   6)          7498E+00        .1932E+00        3892E+01
B(   7)          7023E+00        1932E+00         .3636E+01
B(   8)        -  8827E+00        1932E+00       -.4569E+01
B(  10)         .3502E+00        .1932E+00        1813E+01
B(  11)        -  1170E+01        .1932E+00       -.6056E+01


          ****************************
          ANOVA FOR THE PRESENT MODEL
          ****************************
Source    DOF        Sum Square     Mean Square       F-Value
MODEL     9           249E+04        .276E+03          .320E+04
```

FIT	6.	.607E+01	.101E+01	.117E+02
ERROR	4	346E+00	.864E-01	
TOTAL	19.	.249E+04	.131E+03	